COMPARATIVE ANALYSIS OF THE MORPHOLOGY AND MATERIALS PROPERTIES OF PINNIPED VIBRISSAE

A Thesis

by

CARLY C. GINTER

Submitted to the Office of Graduate Studies of
Texas A&M University
in partial fulfillment of the requirements for the degree of

MASTER OF SCIENCE

December 2011

Major Subject: Wildlife and Fisheries Sciences

Comparative Analysis of the Morphology and Materials Properties of Pinniped Vibrissae

COMPARATIVE ANALYSIS OF THE MORPHOLOGY AND MATERIALS PROPERTIES OF PINNIPED VIBRISSAE

A Thesis

by

CARLY C. GINTER

Submitted to the Office of Graduate Studies of
Texas A&M University
in partial fulfillment of the requirements for the degree of

MASTER OF SCIENCE

Approved by:

Chair of Committee,	Christopher D. Marshall
Committee Members,	Thomas J. DeWitt
	Sudeep Ingole
Head of Department,	John B. Carey

December 2011

Major Subject: Wildlife and Fisheries Sciences

ABSTRACT

Comparative Analysis of the Morphology and Materials Properties of Pinniped
Vibrissae. (December 2011)
Carly C. Ginter, B.S., West Chester University
Chair of Advisory Committee: Dr. Christopher D. Marshall

Vibrissae (whiskers) are important components of the mammalian tactile sensory system, and primarily function as detectors of environmental vibrotactile cues. Pinnipeds possess the largest and most highly innervated vibrissae among mammals and their vibrissae demonstrate a diversity of shapes and likely mechanical properties. These two characteristics are important for vibrotactile sensory perception.

Vibrissae of most phocid seals exhibit a beaded morphology with repeated sequences of crests and troughs along their length. I comparatively characterized differences in vibrissae morphologies among phocid species with a beaded profile, phocid species with a smooth profile, and otariids with a smooth profile using traditional and geometric morphometric methods to test the hypothesis that vibrissal morphologies are species-specific manipulations of a common pattern. The traditional and geometric morphometric datasets were subsequently combined by mathematically scaling each to true rank, followed by a single eigendecomposition. Quadratic discriminant function analysis demonstrated that 79.3, 97.8 and 100% of individuals could be correctly classified to taxon based on vibrissal shape variables in the traditional, geometric and combined morphometric analyses, respectively. At least three separate morphologies were identified since phocids with beaded vibrissae, phocids with smooth vibrissae, and otariids each occupied distinct morphospace in the geometric morphometric and combined data analyses.

Another important characteristic that influences the transduction of vibrotactile information to the mechanoreceptors in the follicle-sinus complex is the materials properties of the vibrissae. Vibrissae were modeled as cantilever beams and flexural stiffness (EI) was measured to test the hypotheses that the shape of beaded vibrissae reduces flexural stiffness and that vibrissae are anisotropic (orientations differ in EI). Species were significantly different and smooth vibrissae were generally stiffer than beaded vibrissae. Beaded vibrissae decrease vibrations in flow, which, combined with lower flexural stiffness values, may enhance detection of small changes in flow from swimming prey. The anterior plane of the vibrissae is likely the most biologically significant in tracking hydrodynamic trails but had lower flexural stiffness values than the dorsoventral orientation. There is likely a complex interaction between shape and mechanical properties in pinniped vibrissae but the ecological and functional implications are currently unknown.

ACKNOWLEDGMENTS

I would like to thank my committee chair, Dr. Christopher Marshall, and my committee members, Dr. Thom DeWitt and Dr. Sudeep Ingole, for their guidance and support throughout the course of my project. Dr. Frank Fish was instrumental in setting me on the path to carry out this research.

This project would not have been possible without the vibrissae samples that were collected by the New Jersey Marine Mammal Stranding Center, Dr. Frank Fish of West Chester University, Dr. Perry Habecker and the University of Pennsylvania New Bolton Center Large Animal Pathology Laboratory staff, Keith Matassa and the University of New England Marine Animal Rehabilitation Center necropsy staff, Lauren Rust and the Marine Mammal Center, Laura Hilbert, Diane Olsen and the animal care staff at Moody Gardens, Alex Whiting of the Native Village of Kotzebue, Alaska, Kathy Frost of the University of Alaska, Fairbanks, Gay Sheffield, Anna Bryan and Lori Quakenbush of Alaska Department of Fish and Game, Brandon Russell at Vancouver Aquarium, Dr. David Rosen of the University of British Columbia, Dr. Stephen Raverty of Ministry of Agriculture and Lands, British Columbia, Canada, Dr. Randall Davis of Texas A&M University and Dr. Terrie Williams of the University of California, Santa Cruz. All samples were collected under a NMFS Southeast Regional Office salvage permit letter to CDM and NMFS permits #358-1585 and 358-1787 issued to the Alaska Department of Fish and Game.

Thanks go to Glenn Gailey for writing the Excel macro that initially saved me hours of data manipulation time. Thanks also to Rajeshwari Paluri for technical assistance with materials testing sample holders. Nathan Furey patiently assisted with making the GIS map of sample collection locations. I am appreciative of helpful discussions of materials testing results with Dr. Betty Sindelar. Thanks to Brian Kot for the graduate school advice, field experience, comic relief and editing of unfunded proposals and essays.

The Department of Marine Biology provided much needed and appreciated funding and logistical support. Additional funding was provided by a Texas A&M University Regent's Fellowship and the Erma Lee and Luke Mooney Graduate Student Travel Grant Fund.

I am grateful to Steve Summarell for providing the MTS sample holders free of charge and for supporting my endeavors in so many ways over the past two years. Finally, I am thankful for the support of my fellow graduate students, friends and family who encouraged me from near and far at every step in this process. Thank you to my "Galveston family" for the laughs, commiserating and encouragement, and to the Summarell family for cheering me on. I could not have accomplished what I have without the constant support of my family, my parents Steve and JoAnn and my sister Stephanie, who have always believed in me.

NOMENCLATURE

cm	centimeters
DFA	discriminant function analysis
E	Young’s Modulus of Elasticity
EFA	elliptic Fourier analysis
EI	flexural stiffness
I	second moment of area
m	meters
MANOVA	multivariate analysis of variance
mm	millimeters
MTS	Materials Testing System
N	Newtons
NMFS	National Marine Fisheries Service
PCA	principal components analysis
QDFA	quadratic discriminant function analysis
s	seconds

TABLE OF CONTENTS

CHAPTER Page

LIST OF FIGURES

LIST OF TABLES

CHAPTER I

INTRODUCTION AND LITERATURE REVIEW

Background

Mammalian vibrissae are specialized hairs that are usually located on face and head, but can be found throughout the body. Most work has focused on mystacial vibrissae, which are located just ventral and lateral to the nares. Whiskers are comprised of a specialized follicle filled with a series of blood sinuses (termed a follicle-sinus complex or F-SC) and mechanoreceptors that reside on specialized tissues surrounding a hair shaft. The hair shaft originates with the F-SC, passes through its center and extends away from the body to interact with the environment. Rats have about 150-200 axons innervating each whisker; cats have slightly more and monkeys have slightly less (Halata and Munger 1980; Lichtenstein et al. 1990; Rice et al. 1986). In general, most aquatic mammals have a similar amount of innervation to terrestrial mammals (Dehnhardt et al. 1999; Hyvärinen 1995; Ling 1977; Reep et al. 2001). Estimates for cetaceans were 40-290 axons per F-SC (Ling 1977). The manatee (*Trichechus manatus latirostris*) and the semi-aquatic Australian water rat (*Hydromys chrysogaster*) both have about 110,000 axons innervating the entire mystacial vibrissae array (Dehnhardt et al. 1999; Reep et al. 2001). Displacement of the hair shaft external to the follicle leads to compression of the mechanoreceptors on the leading edge of the deflection and stretching of the mechanoreceptors on all other sides of the mesenchymal sheath within the F-SC (Rice et al. 1986; Lichtenstein et al. 1990). Extremely dense and sensitive mechanoreceptors in the vibrissae follicle-sinus complexes respond to vibration or bending (Burgess and Perl 1973; Gottschaldt et al. 1973; Halata 1975; Rice et al. 1986; Stephens et al. 1973). Afferent fibers innervating the vibrissae detect parameters of deflection such as amplitude, velocity, duration, frequency and angular direction

---

This thesis follows the style of Journal of Mammalogy.

(Lichtenstein et al. 1990). Laboratory rat (*Rattus rattus*) vibrissal hair shafts have been shown to exhibit a resonance when brushed past an object. The vibrissal array represents a resonance analyzer, with shorter vibrissae tuned to different resonances than longer vibrissae (Hartmann et al. 2003; Neimark et al. 2003; Mitchinson et al. 2004). Recent studies have begun to relate the conical shape of rat vibrissae and the range of overall lengths in the vibrissal array to their resonance and mechanical properties (Carl et al. 2011).

Pinnipeds (seals, sea lions and walruses) have the largest vibrissae among mammals (Dykes 1975; Ling 1977). The mystacial vibrissae differ in number, arrangement and shape among the three groups of pinnipeds: phocids (true seals), otariids (fur seals and sea lions) and odobenids (walruses; Ling 1977). Although they are worn down with use, otariids tend to have longer vibrissae than phocids (King 1983). The longest whiskers have been observed in fur seals. A Northern fur seal (*Callorhinus ursinus*) had whiskers up to 330 mm long (Scheffer 1962). The record for the longest whisker belongs to an Antarctic fur seal (*Arctocephalus gazella*), documented at 480 mm (Bonner 1968). Ognev (1935) reported the vibrissae of gray seals (*Halichoerus grypus*) to grow to a length of 110 mm. The longest vibrissae of harp (*Pagophilus groenlandicus*), hooded (*Cystophora cristata*), harbor (*Phoca vitulina*), ringed (*Pusa hispida*), spotted (*Phoca largha*) and gray seals are around 90 – 100 mm (see Chapter II; Yablokov and Klevezal 1964), although mean length including all vibrissae on the muzzle is much lower (Ginter et al. 2010). Walruses (*Odobenus rosmarus*; the only living odobenid) have shorter and thicker vibrissae than phocids or otariids, at approximately 65 mm long and 3 mm wide (Yablokov and Klevezal 1964). The vibrissal system of pinnipeds is the most derived among mammals, which suggests its importance in sensory reception and processing.

Follicle-Sinus Complex Morphology and Function

Although there are few comparative data, the vibrissal F-SC of pinnipeds differ from terrestrial mammals in that the blood sinus system is tripartite with a ring sinus located between a lower and upper cavernous sinus (Hyvärinen 1989; Hyvärinen and Katajisto 1984; Ling 1966, 1972; Marshall et al. 2006; Stephens et al. 1973). In pinnipeds only the lower cavernous sinus and ring sinus are innervated. Pinnipeds have a much greater investment of innervation to the mystacial vibrissal array than terrestrial or other aquatic mammals. A harp seal vibrissa is innervated by five bundles of nerve fibers, each containing 40-290 individual axons. A total of approximately 20,800-162,400 individual axons connect to the whole vibrissal pad (Ling 1977; Yablokov and Klevezal 1964). This degree of innervation is similar to other mammals, such as cats (Rice et al. 1986). However, ringed seals have more than 150,000 axons innervating the vibrissal array (Hyvärinen 1995). Bearded (*Erignathus barbatus*) seals have the highest number of axons per whisker and innervation to the mystacial pad (197,884-402,600 axons to the whole vibrissal pad) of any mammals described to date (Marshall et al. 2006). The high degree of innervation in pinniped vibrissae results in tactile resolving ability equal to a prehensile tactile organ, such as a monkey's hand (Dehnhardt and Kaminski 1995). The high innervation of California sea lion (*Zalophus californianus*) vibrissae led Stephens et al. (1973) to suggest the importance of sensory reception and interpretation of vibrations in water.

Physical contact or exposure to air or water currents is necessary to activate the receptors in the vibrissae follicle (Dykes 1975). The follicle-sinus complexes of pinnipeds function similarly to other mammals. Most of the nerve fibers that enter the F-SC end at mechanoreceptors connected to the glassy membrane in the ring sinus (Hyvärinen 1989). The lanceolate nerve endings on top of the glassy membrane and Merkel-neurite complexes below the glassy membrane respond to displacement of the hair (Hyvärinen 1989). Merkel endings are compressed between the hair shaft and the glassy membrane by deflection of the hairs (Gottschaldt et al. 1973; Rice et al. 1986) and lanceolate endings are hypothesized to detect acceleration and deceleration of the hair shaft during deflection (Marshall et al. 2006; Rice et al. 1986). Vibrations transmitted by the hair shaft are received by the laminated corpuscles below the ring sinus, which detect stretching and compression to initiate a neural response (Marshall et al. 2006;

Stephens et al. 1973). The upper cavernosal sinus, unique to pinnipeds, can comprise up to 60% of the follicle length and is hypothesized to be a thermal insulator for the mechanoreceptors in the F-SC (Dehnhardt et al. 1998b; Hyvärinen 1995; Marshall et al. 2006; Mauck et al. 2000). The surface temperature of harbor seals' vibrissae pads are kept at as much as 25˚C above ambient air temperature, while other areas of the head had surface temperatures of 2.7-6.0˚C (Dehnhardt et al. 1998b). However, only locations of vibrissal follicles were heated above 19˚C (Mauck et al. 2000). The vibrissal follicle is the functional site of the vibrissal sensory system. However, differences in the morphology and materials properties of the hair shaft would likely affect the signal that is transmitted to mechanoreceptors in the F-SC.

Vibrissal Hair Shaft Morphology and Function

Pinnipeds have either smooth, ellipsoidal vibrissae or vibrissae with a sinusoidal beaded profile, showing a regularly repeating sequence of crests and troughs (Dehnhardt and Kaminski 1995; Ginter et al. 2010; Ling 1977; Watkins and Wartzok 1985; Yablokov and Klevezal 1964). All species of phocid seals, except bearded and monk (*Monachus* sp.) seals, have a sinusoidal beaded profile to their mystacial vibrissal hair shafts (Dehnhardt and Kaminski 1995; Hyvärinen and Katajisto 1984; King 1983; Marshall et al. 2006; Ognev 1935). The literature is inconsistent for Ross (*Ommatophoca rossi*) seal vibrissae (King 1969; Ling 1972; Polkey and Bonner 1966) but they are traditionally grouped with the beaded-whiskered phocid species. A possible factor influencing the presence of bumps on some phocid vibrissae is the growth rate and periodic shedding of the vibrissae and follicles, which was documented in detail for gray seals (Greaves et al. 2004) and harbor seals (Hirons et al. 2001). Gray seal vibrissae were observed to grow in spurts, rather than continuously (Greaves et al. 2004). Vibrissae are not shed with the rest of the pelage in an annual molt, but rather individually and irregularly throughout the year (Ling 1966, 1977). This periodic and intermittent shedding and re-growth of vibrissae likely serves to avoid a decrease in sensory capability if all vibrissae were shed simultaneously or due to vibrissae loss or physical damage (Greaves et al. 2004; Hirons et al. 2001; Ling 1977). In fact the divergence of the vibrissae from the shedding cycle of the pelage underscores the functional significance of this sensory system.

"Most probably the vibrissa is a long sensory lever, where the slightest vibrations in the external portion immediately are transmitted to the internal part, and thus to the nerve endings" (Yablokov and Klevezal 1964). The sinusoidal beaded morphology is hypothesized to enhance prey detection and perhaps navigation in ringed and harbor seals (Dehnhardt et al. 1998a; Dehnhardt et al. 2001; Hyvärinen and Katajisto 1984; King 1983; Ognev 1935; Oliver 1977; Schulte-Pelkum et al. 2007). Beaded phocid vibrissae are a hydrodynamic receptor system (Bleckmann 1994; Hanke and Bleckmann 2004). Although streamlining is the most efficient shape for moving through fluid, recent studies suggest that a bumpy leading edge may actually function to reduce drag more than a smooth leading edge (Fish et al. 2008; Miklosovic et al. 2004). For example, humpback whale (*Megaptera novaeangliae*) flippers possess tubercles, which create a bumpy profile along the leading edge (Winn and Reichley 1985). This morphology has been shown to affect the hydrodynamic characteristics of the flipper to increase maneuverability during turning by decreasing drag and increasing lift forces, even at high angles of attack (Fish et al. 2008; Miklosovic et al. 2004). The beaded profile of phocid vibrissae has been shown to have similar hydrodynamic implications (Hanke et al. 2010). Drag reduction of the vibrissae is necessary in order to keep these thin, flexible structures protracted and therefore able to detect hydrodynamic stimuli in flow. The vibrissae vibrate at a frequency related to the flow of water over them as the seal swims (Hyvärinen and Katajisto 1984). The vibration frequency is related to the mechanical properties of vibrissae, which have not previously been explored (see Chapter III). However, it has been demonstrated by captive animal testing and computational fluid dynamics (CFD) modeling that the beaded profile of the vibrissae decreases vibrations due to ambient flow, compared to a smooth vibrissa (Hanke et al. 2010). A decrease in the vibrations due to ambient environmental noise could make the vibrissae more sensitive to other flow stimuli.

Studies of the tactile discrimination abilities of pinnipeds using mystacial vibrissae (whiskers) have demonstrated that this is an important sensory system. Walruses can discriminate between two different shaped discs down to a surface area of 0.4 cm^2 using only their mystacial vibrissae (Kastelein and Van Gaalen 1988). Tactile discrimination capability of harbor seals, as measured by Weber fraction (c), demonstrated that these seals' vibrissae have resolving power (c = 0.08 – 0.13) similar to a monkey's hand (c = 0.10) (Dehnhardt and Kaminski 1995). Additionally, active touch discrimination using these whiskers has a threshold similar to pinniped vision, which has a Weber fraction estimated to be around 0.06 (Dehnhardt and Kaminski 1995; Schusterman et al. 1965; Wartzok and Ray 1976). California sea lions had slightly higher Weber fractions of 0.24 – 0.26 using their mystacial vibrissae in active discrimination behavior but their responses followed Weber's law as closely as vision (Dehnhardt 1994; Dehnhardt and Dücker 1996). A gray seal appeared to rely on its vibrissae to detect tactile cues and avoid obstacles while swimming through a maze in the dark with visual cues all but eliminated (Oliver 1977). It has been demonstrated that swimming fish create complex hydrodynamic vortex trails (Bleckmann et al. 1991; Blickhan et al. 1992; Drucker and Lauder 1999). These trails induce a change in water velocity that is above the threshold of hydrodynamic reception by most organisms for several minutes, which suggests that swimming fish could be pursued by their predators by detecting and following the hydrodynamic signal the fish leaves in its wake (Hanke et al. 2000). This expands upon the theory that pinnipeds use tactile cues to find prey by suggesting that direct touch may not be necessary for vibrissae function.

Studies showed that harbor seals were able to use mystacial vibrissae to follow the course of a hydrodynamic trail similar to one that a swimming 30 cm fish would create, as well as a trail created by another swimming seal, even if they were blindfolded and auditory cues were eliminated (Dehnhardt et al. 2001; Schulte-Pelkum et al. 2007; Wieskotten et al. 2010b). These data were further supported by control experiments where the whiskers were impeded by placing a stocking mask over the muzzle; the seal was never able to detect the trail. California sea lions, which possess smooth vibrissae, were also able to follow a hydrodynamic trail, but had only a 50% success rate when following a trail with a directional change (Gläser et al. 2011). Additionally, a sea lion showed a drastic decrease in successful tracking when there was a delay of more than a few seconds between trail generation and the start of tracking behavior (Gläser et al. 2011). These results, combined with studies of visual capability, suggest that sea lions are likely able to rely primarily on vision while foraging and therefore may have not developed either the needed bumpy profile of the vibrissal hair shafts and/or the investment of mechanoreceptors and dense innervation to the degree that phocids have.

The concept that pinnipeds rely primarily upon the vibrissal sensory system while foraging in darkness, when vision is of little use, is supported by accounts of blind, wild seals that appeared to be in good health and foraging successfully (Dehnhardt and Kaminski 1995; Hyvärinen 1989; Newby et al. 1970). Newby et al. (1970) observed lactating mother harbor seals that were determined to be blind by their opaque corneas. Lactation is energetically demanding, with female harbor seals losing 80% of their stored fat over the first 19 days of lactation (Boness et al. 1994). If blind seals were unable to find an adequate amount of food with high enough nutritional quality, it is highly unlikely that they would be able to successfully nurse a pup. Miller (1975) compared facial expressions and social interactions in fur seals (*Arctocephalus forsteri*) and walruses. He concluded that while vibrissae may have some social function, they are primarily tactile adaptations for food and object manipulation in water (Miller 1975). The smooth, thick, dense vibrissae of the bearded seal are used as tactile aids in identifying benthic prey (Ognev 1935). Monk (*Monachus* spp.) seals, which also do not show the beaded profile, are opportunistic foraging generalists, with the Hawaiian subspecies (*M. schauinslandi*) hunting primarily benthic prey on coral reefs and the Mediterranean subspecies (*M. monachus*) consuming mostly cephalopods (Goodman-Lowe 1998; Longenecker 2010; Salman et al. 2001). Animal-borne video cameras showed that monk seals foraging over sand kept their smooth vibrissae in nearly constant contact with the substrate (Parrish et al. 2000). Southern sea lions (*Otaria byronia*) were observed to swim underwater with erect vibrissae in contact with the sea bottom

(Dehnhardt and Kaminski 1995; Lindt 1956). However, elephant (*Mirounga* spp.) and Weddell (*Leptonychotes weddellii*) seals possess beaded vibrissae but forage frequently on benthic prey (Burns et al. 1998; Hindell et al. 1991; Le Boeuf et al. 2000; Plötz et al. 2001). Weddell seals equipped with animal-borne cameras were also observed to use vision while hunting beneath ice by swimming below prey and silhouetting it against the lighter under-ice surface before attacking (Davis et al. 1999). Pinnipeds likely use a combination of sensory modalities to navigate and forage in different environments.

Finding prey in open ocean environments has provided strong selection pressures for marine mammals to develop diverse sensory mechanisms for prey detection. Odontocetes (toothed whales) display a refined sensory capability, echolocation, that allows individuals to interpret fine details of their environment, and objects within that environment, using the echoes of high frequency sound produced by the same individual (Au 2008). However, numerous attempts have failed to find evidence for the use of echolocation by pinnipeds (Schusterman et al. 2000; Wartzok 1984). Auditory cues are known to be used for foraging, traveling, predator avoidance and communication (Schusterman 1981). Harbor and spotted seals have been shown to have good brightness discrimination (Hanke et al. 2009; Scholtyssek et al. 2008; Wartzok and McCormick 1978). Northern elephant seals (*Mirounga angustirostris*) are the deepest diving pinnipeds and exhibit a large range of pupillary dilation, which is known to increase dark adaptation rates in other mammals (Levenson and Schusterman 1997, 1999). Harbor seals' visual acuity is approximately equal in air and clear water and these marine mammals have a contrast sensitivity adapted for low light, similar to other carnivores (Hanke and Dehnhardt 2009; Hanke et al. 2011). However, pinnipeds often hunt in areas where concentrations of plankton and fish are high but water is consequently turbid and the visual acuity of harbor seals decreases rapidly even in moderately turbid water (Weiffen et al. 2006). Ringed seals in Lake Saimaa live in murky water under ice cover where the visibility can be reduced to 2 m (Hyvärinen 1989). This illustrates the need for a sensory modality, such as tactile reception by vibrissae, that could compensate for the lack of visual stimuli under commonly encountered foraging conditions (Weiffen et al. 2006). It is likely that pinnipeds use a combination of sight, hearing and vibrissal tactile reception to find, track and capture prey. For example, sea lions may locate the approximate position of a fish using auditory cues, follow the hydrodynamic trail using their vibrissae and capture the fish when it is seen (Gläser et al. 2011). Foraging Weddell seals often only protract their vibrissae in the final stages of an attack (Davis et al. 1999). The complex interaction and relative importance of pinniped sensory modalities in different environments remain to be explored. However, the high innervation, variety of shapes and evidence of hydrodynamic function in pinniped mystacial vibrissae all suggest the importance of this sensory system. This thesis examines the variety of shapes seen in pinniped vibrissae and their mechanical performance since both of these factors likely have functional and ecological implications.

Morphometrics – Shape Analysis

Geometric morphometrics is a relatively new morphological methodology that quantifies and statistically analyzes shape variation and covariation among samples (Adams et al. 2004; Rohlf and Marcus 1993). While traditional morphometrics uses multivariate statistical analysis of a set of variables, which are usually linear distances on an organism, to define shape (Rohlf and Marcus 1993), geometric morphometrics preserves the geometry of a shape and has gained popularity in biological studies in recent years (Adams et al. 2004; Rohlf and Marcus 1993). Within the field of geometric morphometrics there are two general methodologies, landmark-based, which uses homologous biologically definable locations on various specimens, and outline-based, which uses the coordinates of points around the bounding of the specimen. Both methodologies generate shape variables that can be analyzed using multivariate statistics to provide a quantitative description of shape. Outline-based morphometrics often uses elliptic Fourier analysis (EFA) to compare profile shapes and provide a precise and accurate description of shape over a range of size scales (Kuhl and Giardina 1982; McLellan and Endler 1998). Elliptic Fourier analysis allows quantitative description of shape variation by creating four Fourier coefficients for each harmonic in a series of harmonics that are subsequently added to an ellipse to reproduce digitized outlines (see Chapter II). These Fourier coefficients are shape variables that can be statistically analyzed using multivariate methods, such as Principal Components Analysis (PCA). Principal components analysis is useful to reduce a large number of variables down to a more manageable number that still summarizes the majority of the variance within the dataset. A combination of traditional and geometric morphometrics can be used to create a complete, quantified description of shape. Traditional, geometric and a combined methodology were used in this study to quantitatively analyze the different shapes of pinniped vibrissae (Chapter II).

Materials Properties – Flexural Stiffness (EI)

The higher density of water compared to air results in considerable mechanical resistance on the whiskers as an aquatic animal swims (Dehnhardt et al. 1999). The function of a biological structure depends on its mechanical properties, which can be described from an engineering perspective. A property of interest to biologists is Young's modulus of elasticity, which refers to the degree of resistance of a material to deformation under a given load (Etnier 2001; Roark 1943; Vogel 2003; Wainwright et al. 1976). Biological materials demonstrate a broad range of Young's moduli; for example, from $2.1\text{x}10^{-8}$ GPa for a zebrafish larvae superficial neuromast in the lateral line to 84 GPa for human enamel (Craig et al. 1961; McHenry and van Netten 2007). Considerable work has been done to quantify the materials properties of plants. Timber has a broad range of E values (4-16 GPa), depending on whether it is a hardwood or softwood, branch or trunk and tested green or air-dried (Bodig and Jayne 1982; Cannell and Morgan 1987). Cortical bone has much higher E values, ranging from 8 to 24 GPa (Meyers et al. 2008). Another property of interest to biologists is flexural stiffness (EI), which is the product of Young's modulus and a parameter describing the geometry or arrangement of material (Vogel 2003; Wainwright et al. 1976). Flexural stiffness (EI) is the measure quantified in Chapter III to describe the mechanical behavior of pinniped vibrissae. Plant stems and leaf petioles have EI values ranging from $7.3\text{x}10^{-11}$ N/mm^2 to $2.53\text{x}10^{-6}$ N/mm^2 (Ennos 1993; Ennos et al. 2000; Etnier 2003; Etnier and Vogel 2000; Niklas 1991; Vogel 1992). These plant structures have diameter values in the same order of magnitude as pinniped vibrissae. The skeletons of corals, which also have diameter values within the order of magnitude of pinniped vibrissae, have EI values ranging from $7.31\text{x}10^{-9}$ to $1.14\text{x}10^{-7}$ N/mm^2 (Esford and Lewis 1990; Jeyasuria and Lewis 1987; Kim et al. 1992). Scots pine (*Pinus sylvestris*) was found to have much higher EI values ranging from $4\text{x}10^{7}$ - $7.13\text{x}10^{11}$ (Mencuccini et al. 1997). However, the diameter range for these tree samples was 68 – 348 mm, several orders of magnitude larger than pinniped vibrissae (Mencuccini et al. 1997). Although a variety of biological structures have been evaluated in terms of both Young's modulus and flexural stiffness, this thesis is the first attempt to measure the flexural stiffness of pinniped vibrissae.

Objectives and Hypotheses

The objectives of this study were to 1) characterize the morphology and shape of pinniped vibrissae using traditional and geometric morphometrics, and 2) characterize the materials properties of pinniped vibrissae, and model the bending mechanics according to beam theory. I hypothesized that that the morphology and shape of phocid seal whiskers are species-specific, and that these differences are based on manipulations of a similar overall morphological and shape pattern. It was predicted that in statistical analyses, the phocids with smooth vibrissae would cluster with otariids, and be separated from phocids with beaded vibrissae. I also hypothesized that a beaded profile would reduce flexural stiffness compared to smooth vibrissae, and that vibrissal hair shafts are not isotropic, resulting in greater stiffness in some orientations than others.

Samples

Whole vibrissae pads were collected from dead, stranded individuals on the East and West coasts of the United States and from animals taken during legal indigenous hunts in Alaska (Fig. 1). Additional individual vibrissae were opportunistically collected when shed by live, captive animals. Several vibrissae samples from Southern Hemisphere (South America and Antarctica) pinnipeds were collected by colleagues conducting unrelated research in those locations. Vibrissae from six phocid species with beaded vibrissae, one phocid species with smooth vibrissae and five otariid species with smooth vibrissae were analyzed in this study. Samples were collected under a National Marine Fisheries Service (NMFS) Southeast Regional Office salvage permit letter and NMFS permits #358-1585 and 358-1787 issued to the Alaska Department of Fish and Game.

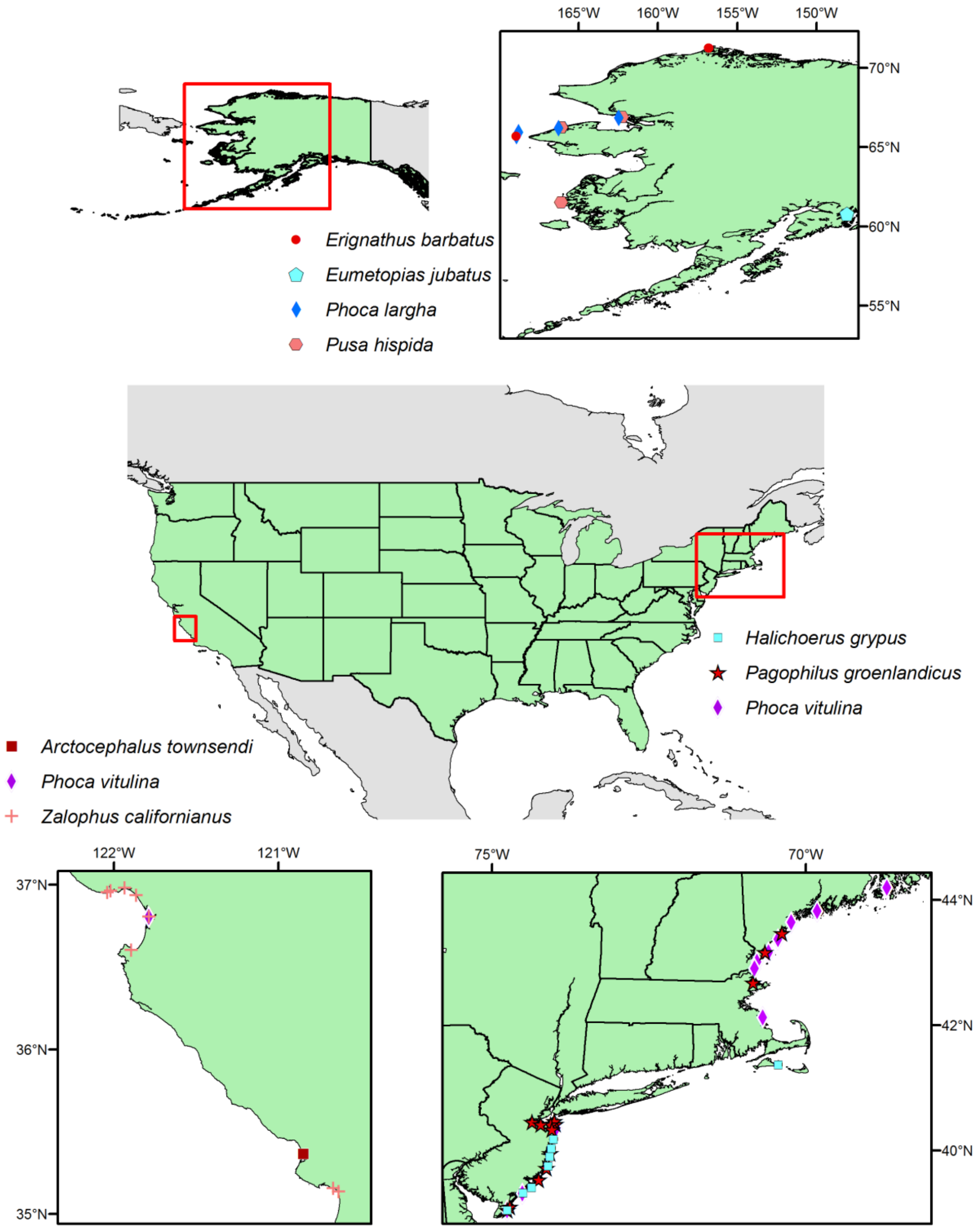

Figure 1. Map of sample collection locations. Individual pinnipeds whose vibrissae were included in this study are represented. Different species are indicated by the different symbols.

CHAPTER II

MORPHOLOGY

Introduction

Many organisms possess highly sensitive mechanosensory structures to monitor and detect physical cues in their environment. Mammalian vibrissae (whiskers) are finely tuned sensory structures. The vibrissae include a follicle-sinus complex (F-SC) with numerous and various types of mechanoreceptors within its complex microstructure and a vibrissal hair shaft that transmits vibrotactile environmental stimuli to these mechanoreceptors deep in the F-SC (Burgess and Perl 1973; Dykes 1975; Gottschaldt et al. 1973; Halata 1975). Although most mammals possess vibrissae, the majority of our knowledge regarding their function is limited to laboratory animals (Ahl 1986; Rice et al. 1997; Rice et al. 1986; Rice and Munger 1986). The number, geometric arrangement, size, morphology, shape and stiffness of vibrissae vary widely among mammals (Ling 1977). Pinnipeds (seals, sea lions and walruses) possess the largest vibrissae among mammals (e.g., Antarctic fur seals (*Arctocephalus gazella*) have vibrissae up to 480 mm long; Bonner 1968) and exhibit a diversity of shapes in these structures (King 1983; Ling 1977; Watkins and Wartzok 1985). In particular, the mystacial vibrissae of phocid seals, with the exception of bearded (*Erignathus barbatus*) and monk (*Monachus* spp.) seals, show a repeating sequence of crests and troughs along their length, giving them a beaded appearance (Dehnhardt and Kaminski 1995; Ginter et al. 2010; Hyvärinen and Katajisto 1984; King 1983; Marshall et al. 2006; Ognev 1935; Watkins and Wartzok 1985).

Many mammals, terrestrial and aquatic, use vibrissae for active touch and other discrimination tasks. However, no other mammal exhibits the unusual beaded vibrissal morphology possessed by most phocid seals. Since vision is a limited sensory modality in aquatic habitats, it follows that marine mammals may have experienced strong selection for compensatory sensory adaptations that facilitate functions such as prey detection, particularly when foraging at night, in turbid water or when diving deeply. Whereas odontocetes (toothed whales) evolved echolocation, pinnipeds have highly derived vibrissal sensory systems (Dehnhardt et al. 1998a; Dehnhardt et al. 2001; Hanke et al. 2011; Hyvärinen 1989; Hyvärinen and Katajisto 1984; Weiffen et al. 2006). Reports of healthy but blind seals foraging successfully in the wild suggest the importance of this sensory system for the aquatic environment (Dehnhardt and Kaminski 1995; Newby et al. 1970). Experimental evidence has shown that phocid seals rely heavily upon their vibrissae to follow hydrodynamic trails (Dehnhardt et al. 1998a; Dehnhardt et al. 2001; Schulte-Pelkum et al. 2007; Wieskotten et al. 2010a, 2010b), as well as to orient themselves when vision is restricted (Wartzok et al. 1992).

The distinctive shape of phocid seal vibrissae, with a sinusoidal beaded profile, has been shown to decrease vibrations during ambient flow while the seal is swimming, compared to smooth vibrissae (Hanke et al. 2010). Previous morphological analyses of phocid vibrissae demonstrated species-specific differences (Ginter et al. 2010). However, there are few quantitative data regarding the morphology of phocid vibrissae and, to our knowledge, no characterization of their geometry has been conducted. Therefore, I conducted a comparative study on the shape and morphology of pinniped vibrissae. I tested the hypothesis that the beaded morphology of phocid vibrissae is conserved with variants in peak-to-peak distance and crest and trough width representing species-specific differences. I also hypothesized that phocids with beaded vibrissae, phocids with smooth vibrissae and otariids would each occupy distinct morphospace from each other, which may facilitate functional differences with ecological consequences.

Materials and Methods

Mystacial vibrissal hair shafts external to the follicle (hereafter simply termed vibrissae) from 11 pinniped species and 92 individuals were analyzed to quantify shape and morphological differences among species with beaded and smooth profiles (Table 1). Samples were collected from dead, stranded animals in New Jersey, New England

and California, from legal indigenous hunts in Alaska and opportunistically when shed by captive animals. To standardize our comparisons, the longest vibrissae which did not show any wear or breakage from each individual were used. These vibrissae always occurred in the most lateral portions of the lower rows of the mystacial vibrissal field. Scaled digital photographs (27.0 pixels/mm) of whole vibrissae were taken with a Nikon D200 SLR camera. To maximize the contrast between the background and the vibrissa in the photograph, all vibrissae were dyed black (using Revlon ColorSilk hair dye #10; Revlon Cons. Prod. Corp., N.Y., NY 10017). Vibrissae were coated with the dye mixture until the dye had penetrated the hair shaft and would not rinse off with water. Vibrissae were placed on a white background with the laterally flattened side down and held flat by a large glass slide to eliminate shape distortion. The camera was mounted on a photographic copy stand normal to the vibrissa and a remote shutter release was used to trigger imaging.

Table 1. Morphology vibrissae samples. Individual pinnipeds analyzed in this portion of the study are classified by family, species and vibrissal profile.

Vibrissal Profile	Family	Species	Number of Individuals
Beaded	Phocidae	Gray seal (*Halichoerus grypus*)	8
	Phocidae	Harbor seal (*Phoca vitulina*)	15
	Phocidae	Harp seal (*Pagophilus groenlandicus*)	16
	Phocidae	Ringed seal (*Pusa hispida*)	16
	Phocidae	Spotted seal (*Phoca largha*)	9
Smooth	Phocidae	Bearded seal (*Erignathus barbatus*)	10
	Otariidae	California sea lion (*Zalophus californianus*)	12
	Otariidae	Guadalupe fur seal (*Arctocephalus townsendi*)	1
	Otariidae	Northern fur seal (*Callorhinus ursinus*)	2
	Otariidae	South American fur seal (*Arctocephalus australis*)	2
	Otariidae	Steller sea lion (*Eumetopias jubatus*)	1

Traditional morphometric measures were collected using the scaled digital photographs of whole vibrissae following Ginter et al. (2010). Traditional morphometric measurements collected were: peak-to-peak distance (linear distance between successive crests along the dorsal and ventral margins of each vibrissa), crest width (width of beads), trough width (width of constrictions), and curvilinear length of the entire vibrissa (Fig. 2). All measurements were made using ImageJ (version 1.41, National Institutes of Health, Bethesda, MD, USA; http://rsbweb.nih.gov/ij/). Each of the five measurement types was made multiple times on each vibrissa. The values for each type were averaged for each individual vibrissa. The ratio of mean crest width to mean trough width was computed for each species. The geometric mean of all traditional morphometric measures for each individual was used as a standard proxy for overall size in statistical analysis of the traditional morphometrics (Darroch and Mosimann 1985).

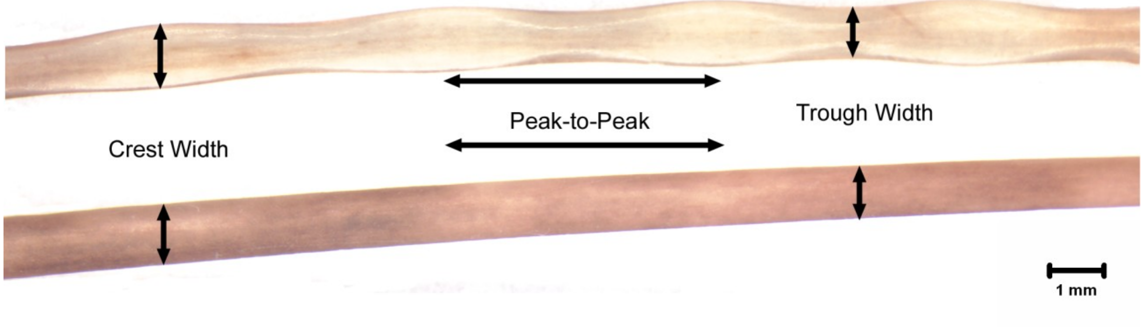

Figure 2. Locations of traditional morphometric measurements on beaded and smooth vibrissae. A ringed seal (top) and California sea lion (bottom) vibrissa are shown with locations of three traditional morphometric measurements (peak-to-peak distance, crest width and trough width) indicated by the black arrows. The measurements are labeled by the text between the two vibrissae. Peak-to-peak distance is not in reference to any physical structures on smooth vibrissae; it is simply the distance between successive measurements of vibrissal width.

I used outline-based, rather than landmark-based, geometric morphometric analysis due to the lack of homologous landmarks on vibrissae. The same images used for the traditional morphometric measurements were thresholded using ImageJ. TpsDig2 software (Rohlf 2004) was used to fit an outline to each thresholded vibrissal image (Fig. 3), calculate the area within the outline, and save the series of X-Y coordinates for each outline. The coordinates were renumbered using a Microsoft Excel 2007 algorithm to standardize the location of "point 1" at the middle of the base of each vibrissa. The renumbered coordinates were imported to EFAWin software (Rohlf 1993) for Elliptic Fourier Analysis (EFA). Harmonics were added sequentially until digital reconstructions of the vibrissae outlines were judged by eye to completely represent the outlines of all vibrissae in this study. Good fit was apparent with 15 harmonics. The shape variables that resulted were set to be invariant to size (area of the first harmonic ellipse), orientation, and rotation. Area of the first ellipse is a reasonable and accepted standard for calculating subsequent harmonic coefficients. However, area within the outline, measured in pixels using tpsDig2, was used as a more biologically relevant measure of size in our statistical analyses.

Elliptic Fourier harmonic coefficients and the log transformed traditional morphometric measures were combined to create a more complete analysis of vibrissal form. However, since the two methods measured vibrissae in different units, the scale of each dataset was converted to match their true rank to be comparable. Matrix rank is the number of linearly independent columns or rows in a data matrix (Pavlicev et al. 2009). In a more practical vein, the true rank is the number of components that collectively summarizes variance above "noise" such as digitization error (Vickerman and Gilmore 2009). Such thresholds are usually set to encompass 95 or 99% of total variance. True rank scaling is accomplished by multiplying each data matrix by the square root of the data's true rank divided by the original variance of the data matrix. Data scaled in this manner can be entered together into a single principle components decomposition (T. J. DeWitt, In prep.).

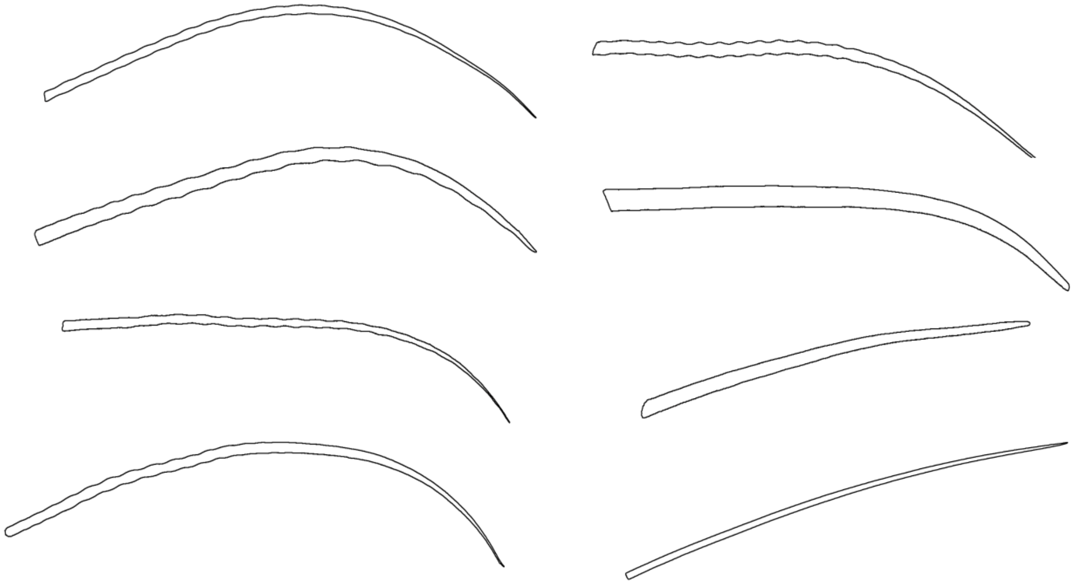

Figure 3. Example outlines of a vibrissa from each species analyzed. Left column from top to bottom: gray, harp, ringed, spotted. Right column from top to bottom: harbor, bearded, fur seal and sea lion.

Statistical Analyses

All statistical analyses used JMP software (version 8.0.1, SAS Institute, Inc., Cary, NC), with the exception of partial η^2, which was calculated using SPSS (version 14.0.1, SPSS Inc.). Discriminant function analysis (DFA) provided a heuristic measure of how well each morphometric method performed in correctly classifying individual pinnipeds to species based on vibrissal shape. Quadratic, as opposed to linear, DFA allows for each taxon to be predicted based on its own variance-covariance matrix in the canonical space. Different covariance structures can result from factors such as small sample sizes (e.g. < 30 individuals per taxon). I ran both types of DFA in each of the three analyses to provide a complete comparative basis for each method. Results of all statistical analyses were considered to be significant at $p<0.05$.

Traditional Morphometrics

All traditional morphometric data were log+1 transformed for normality. Log+1 transformation was used to avoid negative numbers that could not be used in calculation of geometric mean size. Species-specific differences in morphological variation were tested using multivariate analysis of variance (MANOVA) with species, geometric mean and an interaction effect between species and geometric mean as the independent variables and the log-transformed linear distances as the dependent variables. To remove the effect of size in the dataset before evaluating the species effect using DFA, a second MANOVA was run with only geometric mean as the independent variable and the log transformed linear distances as the dependent variables. Residuals from that analysis were subsequently used in both linear and quadratic DFA with the species effect. One-Way ANOVA with Tukey HSD post-hoc tests was used to evaluate differences among species in morphometric measurements on the vibrissae. Such use of ANOVA following MANOVA is referred to as "protected" ANOVA, and is a common practice in ecology and evolutionary biology (Scheiner 2001). However, significance levels for these ANOVA tests should be taken less as precise statements and more as useful heuristic devices, to help distinguish which original variables contribute most strongly to differences between taxa in the multivariate space. These "protected" p-values are demarcated herein using the approximation symbol "≈".

Geometric Morphometrics

The EFA coefficients were compared among species using Principal Components Analysis (PCA) on correlations. Principal components (PCs) on correlations, rather than covariances, were used because small-scale differences in vibrissa morphology were more important in discriminating species than large-scale differences, such as overall curvature. PCs on covariances tend to weight large-scale differences more heavily, while PCs on correlations give all variables equal weight (Jackson 1993). The number of principal components necessary to summarize 99% of the variation in the dataset was used in subsequent analyses. Area within the vibrissal outline was used as the measure of size for the geometric morphometric analysis. Since area is a squared (two dimensional) measurement, the square root of area was taken to convert this value to a linear measurement, which would be comparable to the linear traditional measurements. The square root of area was subsequently log transformed for normality. A MANOVA was run with species, log-transformed square root of vibrissae area and an interaction effect between species and vibrissae area as the independent variables and principal components of Fourier coefficients as the dependent variables. To remove the effect of size in the dataset before conducting DFA, a second MANOVA was run with only log-transformed square root of vibrissae area as the independent variable and principal components summarizing 99% of the variance as the dependent variables. Residuals from that analysis were used in both linear and quadratic DFA with the species effect.

Combined Traditional and Geometric Morphometric Data

To scale each of the morphometric datasets to its true rank, I used eigenvalues of the covariance matrix from the PCA for the traditional morphometric dataset and the correlation matrix from the PCA for the geometric morphometric dataset. True rank was defined as the number of principal components needed to summarize 99% of the variance in each dataset. Once scaled, the datasets were subsequently combined and principal components were generated for the new data matrix. The principal components needed to summarize 99% of the variance in the combined dataset were used as dependent variables in a MANOVA with species, geometric mean, log-transformed square root of vibrissae area, interaction effects between species and each size measure, an interaction effect between the two size measures and a three-way interaction effect between species and both size measures. To remove the effect of size in the dataset before DFA, a second MANOVA was run with only geometric mean and log-transformed square root of vibrissae area as the independent variables and principal components as the dependent variables. Residuals from that analysis were used in linear and quadratic DFA with the species effect.

Results

Traditional Morphometrics

To maintain the comparative aspect of the study, I measured smooth vibrissae, which do not have crests and troughs, at approximate points analogous to the crest and trough locations on beaded vibrissae (Fig. 2). The mean peak-to-peak distance measured along the dorsal and ventral margins of all beaded vibrissae was as a guide to measure width at multiple locations on smooth vibrissae. These width measurements were analogous to crest width on beaded vibrissae. Since smooth vibrissae do not have a sinusoidal profile (i.e., changes in width along the length of the vibrissa), our calculation of the ratio of crest width to trough width was 1 by definition for otariids and bearded seals (Table 2). Although I refer to width values of smooth vibrissae as being crest and trough widths, this nomenclature was used simply to enable comparison with beaded vibrissae and does not describe the shape of smooth vibrissae.

The total length of vibrissae analyzed in this study ranged from 60 mm to 110 mm. The number of beads per cm along the vibrissa ranged from 1.1 (harp seal) to 3.4 (gray seal) and species were significantly different in this variable ($p \approx 0.002$; Table 2). For beaded vibrissae, the mean values for the peak-to-peak distance along the dorsal and ventral vibrissal margins were nearly identical, indicating that the distance between successive crests is not affected by curvature of the overall vibrissa (Table 2, Fig. 4A). Bearded seals had the widest smooth vibrissae and spotted seals (*Phoca largha*) showed the greatest mean crest and trough widths of all beaded vibrissae. The lowest crest and trough widths were seen in ringed seals (*Pusa hispida*; Table 2, Fig. 4B). However, ringed seals had the highest crest width to trough width ratio, indicating that these vibrissae have the most pronounced sinusoidal profile of the five phocid species investigated with beaded vibrissae. Spotted seals had the lowest crest width to trough width ratio, indicating that these seals have the least pronounced sinusoidal profile of the five beaded phocid species. Crest to trough width ratios of harp (*Pagophilus groenlandicus*) and harbor (*Phoca vitulina*) seals were nearly indentical to each other as were the crest to trough width ratios of spotted and gray (*Halichoerus grypus*) seals (Table 2).

Table 2. Results of traditional morphometric measurements. Mean ± SD values for each species are given. Significant differences between species for total length and number of beads per cm are indicated by different letters. Significant differences between species for the other traditional morphometric measurements are given in Figure 3. Species with different letters are significantly different from one another.

	Dorsal Peak-to-Peak Distance (mm)	Ventral Peak-to-Peak Distance (mm)	Crest Width (mm)	Trough Width (mm)	Crest Width / Trough Width	Total Length (mm)	# of Beads / cm
Harp	3.97 ± 0.70	3.94 ± 0.69	0.88 ± 0.14	0.69 ± 0.13	1.28	80.6 ± 10.8^{ab}	2.2 ± 0.4^{bc}
Harbor	3.27 ± 0.39	3.26 ± 0.40	0.92 ± 0.13	0.73 ± 0.12	1.26	86.5 ± 10.5^{ab}	2.3 ± 0.4^{abc}
Ringed	3.56 ± 0.73	3.53 ± 0.72	0.70 ± 0.21	0.49 ± 0.21	1.44	79.6 ± 10.9^{ab}	2.5 ± 0.5^{ab}
Spotted	4.01 ± 0.63	3.99 ± 0.63	1.04 ± 0.15	0.85 ± 0.15	1.22	91.2 ± 7.9^{a}	1.9 ± 0.2^{c}
Gray	3.43 ± 0.38	3.41 ± 0.39	0.76 ± 0.13	0.63 ± 0.11	1.21	73.8 ± 12.5^{b}	2.7 ± 0.5^{a}
Bearded	3.64 ± 0.66	3.62 ± 0.65	1.17 ± 0.28	1.18 ± 0.27	0.99	77.2 ± 9.5^{ab}	0
Fur Seals	3.64 ± 0.66	3.62 ± 0.65	0.97 ± 0.11	0.96 ± 0.12	1.01	83.0 ± 20.3^{ab}	0
Sea Lions	3.64 ± 0.66	3.62 ± 0.65	0.84 ± 0.19	0.84 ± 0.19	1.00	90.7 ± 11.3^{a}	0

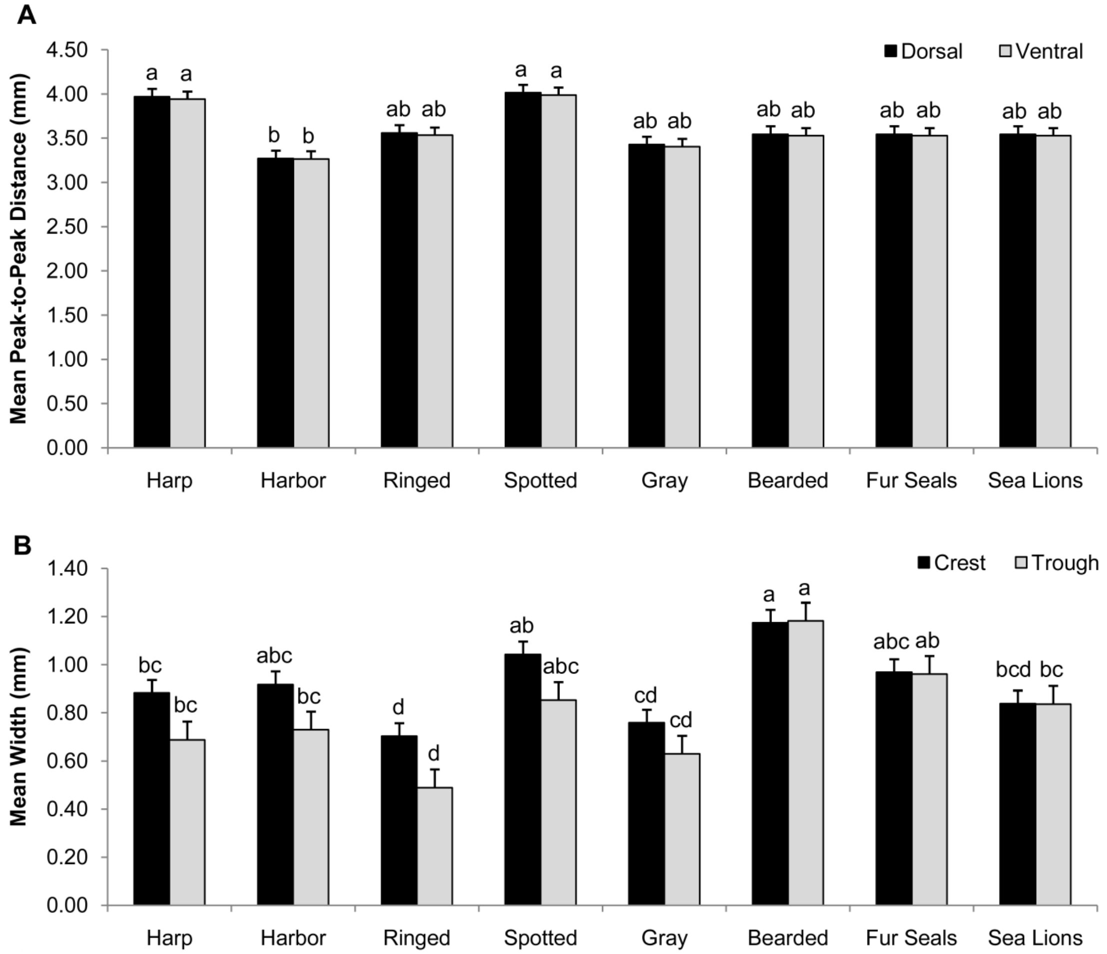

Figure 4. Results of the traditional morphometric measurements. Vibrissae from five species of phocid seals with beaded vibrissae, one species of phocid with smooth vibrissae (bearded) and otariids were analyzed. One-Way ANOVA's were performed following overall significance of species effects in MANOVA. Species with the same letter were not significantly different; species with different letters were significantly different for the given measure (Tukey HSD; $p<0.05$). A) Mean (+SE) peak-to-peak distances along the dorsal and ventral margins of the vibrissa. B) Mean (+SE) crest and trough widths.

There were significant differences between some species in each of the traditional morphometric measurements. ANOVA with Tukey post-hoc results showed that harp and spotted seals significantly differed from harbor seals ($p \approx 0.0035$ and $p \approx 0.0100$, respectively; Fig. 4A) for the log of peak-to-peak distance along the dorsal margin of the vibrissa. The other species did not significantly differ from one another for this variable. Harp and spotted seals also significantly diffed from harbor seals ($p \approx 0.0047$ and $p \approx 0.0128$, respectively) for the log of peak-to-peak distance along the ventral margin of the vibrissa, and the other species did not significantly differ from one another in this variable (Fig. 4A). Bearded seals differed from all species except spotted ($p \approx 0.9643$), harbor ($p \approx 0.1435$) and fur seals ($p \approx 0.8088$) for the crest width variable, and ringed seals differed from all species except sea lions ($p \approx 0.2575$) and gray seals ($p \approx 0.9482$; Fig. 4B). Ringed seals differed from all species except gray seals for the trough width variable ($p \approx 0.0656$), and bearded seals differed from all species except fur ($p \approx 0.8349$) and spotted seals ($p \approx 0.0854$; Fig. 4B). Again, bearded seals, fur seals and sea lions do not have physical crests and troughs so these comparisons refer to their vibrissal width values at points homologous to crests and troughs on beaded vibrissae (Fig. 2). Species were not significantly different in the log length of the vibrissae variable, except for gray seals, which differed from sea lions and spotted seals ($p \approx 0.0205$ and $p \approx 0.0289$, respectively; Table 2). Intraspecific variation could not be effectively assessed due to the low number of individuals per species.

Quadratic DFA on the traditional morphometric measures separated beaded species from non-beaded species on Canonical axis 1 (Fig. 5). In this analysis otariids separated into two groups that slightly overlapped with one another. Bearded seals (smooth vibrissae) overlapped with both gray seals from the beaded phocid cluster and fur seals in the otariid group. Gray seals overlapped only with harbor seals from the beaded phocid cluster. Spotted and harp seals overlapped extensively, while ringed and harbor seals were completely separated from each other. Canonical axis 2 was likely composed of more than one variable and may have separated species primarily based on overall vibrissal length, with harbor seals being further separated from the beaded cluster by their lower peak-to-peak distances (Table 2). Interestingly, gray seals had the highest mean number of beads per cm but were located closer to the smooth-whiskered species in morphospace (Fig. 5). Quadratic DFA showed that the traditional morphometric measures correctly classified 73 out of 92 individuals (79.3%; Table 3).

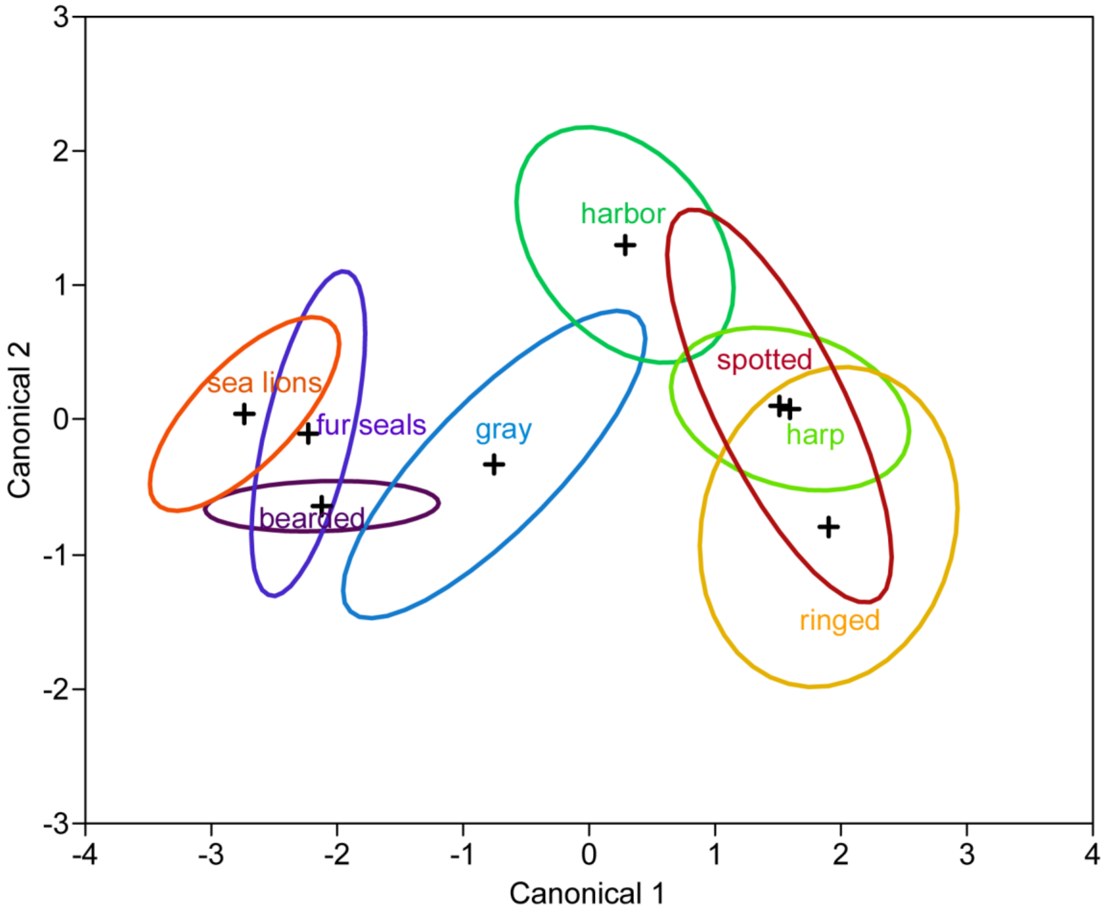

Figure 5. Traditional morphometrics centroid plot. Results of the quadratic discriminant function analysis (QDFA) on the traditional morphometric measurements. Crosses mark the mean for each species; ellipses are 95% confidence regions.

Table 3. MANOVA results for the three analyses. Partial η^2 is a measure of effect strength. LDFA% and QDFA% are the percentages of individuals that were correctly classified by the linear discriminant function analysis and quadratic discriminant function analysis, respectively. Geomsize (geometric mean) and LogSqrtArea (log of the square root of the area) were the measures of vibrissal size.

		F	DF	p	Partial η^2	LDFA %	QDFA %
Traditional	Species	9.2	35,305.3	<0.0001	0.45	64.1	79.3
	Geomsize	6867.5	5,72	<0.0001			
	Species*Geomsize	3.1	35,305.3	<0.0001			
Geometric	Species	2.5	126,397.7	<0.0001	0.42	78.3	97.8
	LogSqrtArea	3.4	18,59	0.0002			
	Species*LogSqrtArea	1.7	126,397.7	<0.0001			
Combined	Species	4.4	133,340.9	<0.0001	0.50	84.8	100.0
	LogSqrtArea	10.1	19,50	<0.0001			
	Geomsize	8.9	19,50	<0.0001			
	Species*LogSqrtArea	2.8	133,340.9	<0.0001			
	Species*Geomsize	2.3	133,340.9	<0.0001			

Geometric Morphometrics

A good (identical by eye) outline fit of each vibrissa was obtained with fifteen harmonics. Four Fourier coefficients (A, B, C, D) were generated to describe each of the 15 harmonics, plus the two zeroth (A0 and C0) harmonics, for a total of 62 shape variables. Fifteen harmonics provided enough variability in shape definitions that eighteen PCs summarized 99% of the variance within the dataset. I therefore used these 18 variables as our metrics of shape in subsequent analyses. Both linear and quadratic DFA provided good discrimination among species based on shape (Table 3). Due to the greater discriminatory ability of quadratic DFA I focused on those results. The quadratic DFA on the geometric morphometric measures separated otariids from phocids (Fig. 6). The phocids with beaded vibrissae clustered together and all species overlapped with each other. Additionally, the otariids separated into two non-overlapping groups, whereas these same groups overlapped slightly in the traditional plot. Bearded seals were positioned between beaded phocids and otariids, but were completely separated from the phocid cluster and both otariid groups, in contrast to the traditional plot. Canonical axis 1 appeared to separate beaded vibrissal species from non-beaded vibrissal species, as seen in the traditional plot. Canonical axis 2 may have separated species based on overall vibrissal length, since sea lions and bearded seals had the longest and shortest smooth vibrissae, respectively, and spotted and gray seals had the longest and shortest beaded vibrissae, respectively (Table 2). Alternatively, this axis may be detecting differences in cross-sectional shape, or an interaction of several shape characteristics. Subsequent canonical axes made only minor contributions to discriminatory ability. Quadratic DFA showed that the principle components of elliptic Fourier harmonic coefficients facilitated classification of 90 out of 92 individuals (97.8%; Table 3).

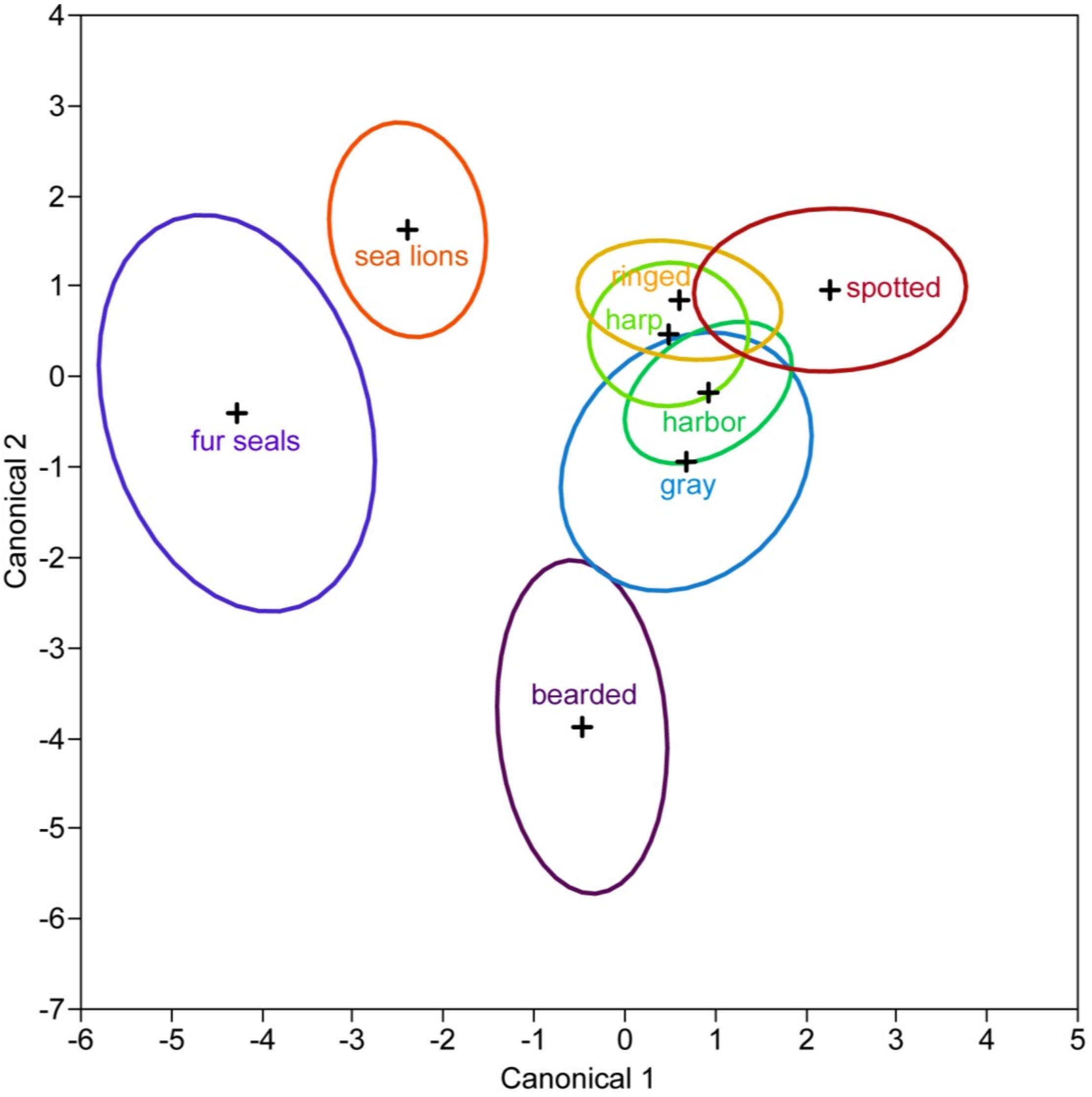

Figure 6. Geometric morphometrics centroid plot. Results of the quadratic discriminant function analysis (QDFA) on the elliptic Fourier harmonic coefficients (geometric morphometrics). Crosses mark the mean for each species; ellipses are 95% confidence regions.

Combined Traditional and Geometric Morphometric Data

The traditional and geometric morphometric data exhibited shared and unique aspects of discriminatory ability. The redundancy (similar taxonomic discrimination) implies a combined analysis is more appropriate, more complete and more powerful. A PCA on the EFA harmonic coefficients showed that eighteen PCs were required to summarize 99% of the variance in the dataset compared to a PCA on the traditional dataset, which only needed three PCs to summarize 99% of the variance in the data. Therefore, the true ranks of the geometric and traditional morphometric datasets were eighteen and three, respectively. If there were no redundancy between the two datasets, a combined, expected 21 PCs would be required to summarize 99% of the variance in the dataset. However, the combined dataset required 19 PCs on correlations to summarize 99% of the variance in the dataset. This showed that there was some overlap between the traditional and geometric morphometric methodologies. The MANOVA results for the combined data are summarized in Table 3. Since two different measures of size were used in the traditional and geometric morphometric analyses, both size measures were included in the combined data model. Insignificant effects were removed from the model.

Quadratic DFA again clearly separated phocids and otariids on Canonical axis 1 with bearded seals occupying an intermediate position between otariids and beaded phocids (Fig. 7). Canonical axis 2 again appeared to separate species in our dataset based on vibrissal length. This separation was clear for the smooth-whiskered species, but the small-scale intricacies of the beaded profile likely complicated the relationships between the beaded phocids. For example, spotted seals had the longest vibrissae but may have been pulled along Canonical axis 2 towards harp seals and away from harbor seals by the peak-to-peak distance variables (Table 2). Surprisingly, gray seals, with the highest mean number of beads per cm, were again pulled towards the smooth-whiskered species. In this analysis, harbor and gray seals did not overlap with either spotted or harp seals, but did overlap with each other and ringed seals. Harp and ringed seals overlapped considerably (Fig. 7). In contrast to the centroid plots for the geometric and traditional morphometrics, otariids loaded higher than phocids on Canonical axis 1 and bearded seals had the highest loading on Canonical axis 2.

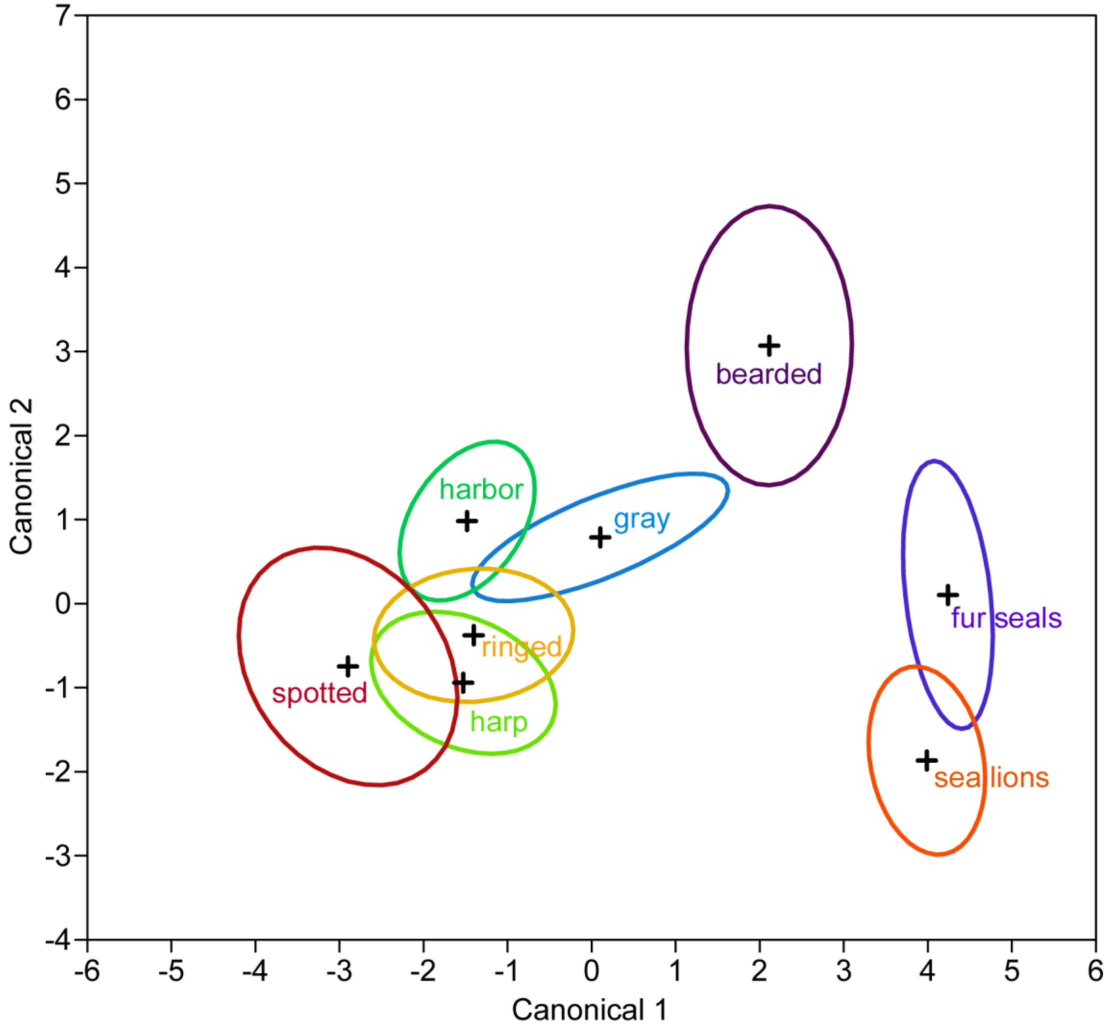

Figure 7. Combined data centroid plot. Results of the quadratic discriminant function analysis (QDFA) on the combined dataset. Crosses mark the mean for each species; ellipses are 95% confidence regions.

Quadratic DFA on the combined dataset correctly classified 100% of individuals (Table 3), compared to 79.3% and 97.8% for the traditional and EFA datasets, respectively. This demonstrated that each method found differences between species that the other method did not. The combined methodology incorported all differences and was the best at correctly classifying species. In all three analyses, quadratic DFA outperformed linear DFA in correctly classifying individuals (Table 3). Since all factors in the statistical models were significant, I compared the proportion of partial variance explained by the main effect of interest, species, using Wilks' partial η^2. This value was similar for all three analyses but highest for the combined dataset (Table 3). This indicates that the species effect was relatively strongest in the combined analysis, and relatively weakest in the geometric morphometric analysis. However, the species effect still explained approximately 50% of the variance in each of the three models.

Individual animals were classified by the recovering stranding network or indigenous group into one of five age classes: pup, yearling, juvenile, subadult or adult. The five age classes did not have significantly different vibrissae lengths ($p=0.0584$) or vibrissae areas ($p=0.1438$). Adults and subadults had significantly higher vibrissal length values than juveniles and yearlings ($p=0.0018$ and $p=0.0012$, respectively), which both had significantly higher vibrissal length values than pups ($p=0.0003$). For overall body length, yearlings and juveniles were not significantly different from each other ($p=0.9998$). Adults and subadults had significantly higher body weight values than the other three age classes ($p<0.0001$). Pups, yearlings and juveniles did not have significantly different body weights ($p=0.0717$). Males and females did not significantly differ in body weight ($p=0.1512$), body length ($p=0.1987$), vibrissal length ($p=0.9169$) or vibrissal area ($p=0.8249$).

Discussion

Phocids with beaded vibrissae show species-specific variation on a common sinusoidal beaded pattern. In all analyses, the phocids possessing beaded vibrissae clustered together. However, it is interesting to note that the only two cogeneric phocids in the study, harbor and spotted seals, did not overlap at all in the combined data analysis and overlapped only partially in the geometric morphometric and traditional morphometric analyses. Gray seals appeared to occupy an intermediate position in morphospace between the other beaded phocids and smooth-whiskered bearded seals in all three analyses. This was surprising since this species had the highest number of beads per cm and the overall shape appeared quite similar to the rest of the beaded phocids. Ginter et al. (2010) initially found a different pattern in traditional morphometric measurements along the vibrissae of gray seals compared to harp and hooded (*Cystophora cristata*) seals, but that difference was not maintained when additional samples were added (C.C. Ginter, unpubl. data). Gray seals possess different head morphology from other phocids. Cameron (1967) and King (1983) described the nose of male gray seals as high and arched, while females have a long, straight profile to the top of the head. Gray seals are similar to hooded and elephant (*Mirounga* sp.) seals in that the males have enlarged snouts used in visual signaling (Miller and Boness 1979). The broader snout may change the position of vibrissae on the muzzle. As a result of this difference in location, vibrissae may have evolved an alternative morphology. While the phocid species with beaded vibrissae always clustered together in morphospace, the fact that all individuals could be correctly classified to the species level demonstrated that the beaded profile is not identical. I sampled a large number of Phocinae species, but not all members of this subfamily were included in the study. However, based on the variation within this beaded vibrissal group, I predict that the rest of family Phocidae would cluster with the beaded phocids examined here.

Bearded seals, a phocid with smooth vibrissae, were positioned between beaded phocids and otariids in morphospace. Interestingly, the centroid ellipses for bearded seals and otariids (which also possess smooth vibrissae) never overlapped in the geometric morphometric or the combined data analysis. In fact, the centroid ellipse for bearded seals was closer in morphospace to the beaded phocids than to the smooth-whiskered otariids in the geometric and combined analyses. This strongly suggests that the smooth vibrissae of bearded seals are different from the smooth vibrissae of otariids in this study. This difference may be related to cross-sectional shape. Bearded seal vibrissae are almost rectangular in cross-section and this shape differs considerably from the oval cross-sectional shape of otariids and other phocids (Marshall et al. 2006; pers. obs.). A limitation of this comparative analysis is that the other phocids with smooth vibrissae, monk seals (*Monachus* spp.), were not included. However, based on personal observations and diet studies in the literature, I predict that monk seals would not occupy the same morphospace as bearded seals. Rather, they may be intermediate between bearded seals and the beaded phocid cluster or intermediate between bearded seals and otariids. The interesting differences among pinniped vibrissae without a beaded profile were a surprising result of this study. I have reported evidence that there may be variation in smooth vibrissal shape and morphology among otariids, since the geometric morphometric approach completely separated otariids into two groups, and the combined data analysis demonstrated only a minimal overlap between these groups. Clearly these differences in morphology and shape previously have been overlooked and may have important ecological consequences.

It is important to note that although the comparisons of vibrissal length and area between genders and among age classes are interesting, full Level A data were only obtained for 45 out of 92 individuals from five species. No morphological data were available for any of the animals classified as subadults. Additionally, more males than females were obtained (34 males vs. 16 females) and there were more known adult males than known adult females, both of which may have biased the results. However, additional support for the observed lack of difference in vibrissal length among age classes comes from Scheffer's (1962) observation of a full term Northern fur seal (*Callorhinus ursinus*) fetus with vibrissae as long as 63 mm and Bonner's (1968) observation of a three week old Antarctic fur seal (*Arctocephalus gazella*) with vibrissae up to about 80 mm long. A four and a half month old Southern elephant seal (*Mirounga leonina*) fetus had mystacial vibrissae up to 27 mm long (Ling 1966). A ringed seal pup of the year in the present study had vibrissae that were slightly longer than the mean value for that species. Although caveats are certain to arise, the data analyzed here suggest that there are no gender or age class effects on vibrissal morphology and shape.

Although I focus on the shape of individual vibrissae here, other factors also are likely to be important in vibrotactile sensory perception, such as location, distribution of the vibrissae on the muzzle, and innervation. The function of the entire mystacial vibrissa pad is most likely an interaction between vibrissal hair shaft shape, the geometry and location of the vibrissae. The interaction of morphology at these two scales is likely to be related to foraging mode and strategy. Bearded seals and walruses exemplify the importance of the geometry of mystacial vibrissae location. The distribution of bearded seal vibrissae differs from other phocids. Instead of lying along the lateral sides of the rostrum, bearded seals have vibrissae widely distributed over the anterior portion of a blunt muscular muzzle (Ling 1977; Marshall et al. 2006). Bearded seals forage for benthic invertebrates (Burns 1981). Walruses, another benthic foraging specialist, exhibit a similar vibrissal distribution (Fay 1982). This vibrissal arrangement is related to a benthic foraging mode and appears to be convergent with the vibrissal arrangement on the oral disk of sirenians, which also spend considerable time foraging on the benthos (Marshall et al. 1998; Marshall et al. 2003; Reep et al. 1998).

Otariids have smooth vibrissae and feed on similar prey to phocids with beaded vibrissae (Pauly et al. 1998), which suggests that beaded vibrissae are not critical in catching certain prey items. However, otariids generally do not dive to the depths that phocids do in search of prey. The greater amount of ambient light present in shallower water may allow otariids to rely more heavily upon vision for prey detection and capture or a combination of visual, auditory and tactile cues (Gläser et al. 2011). Both California sea lions and harbor seals are able to detect water velocities below those that would be generated by a swimming fish using their vibrissae (Dehnhardt and Mauck 2008; Dehnhardt et al. 1998a). However, blindfolded California sea lions could only successfully track a hydrodynamic trail using their vibrissae 50% of the time when the signal made a single turn. There was also a decrease in tracking ability when there was a delay of more than a few seconds between the generation of the trail and the beginning of the sea lion's search for it (Gläser et al. 2011). These performance data suggest that vibrissae are an important sensory modality in this species, but are not the only sensory system involved in prey tracking, since it is unlikely that a chased fish will swim in a straight line.

In contrast, harbor seals are able to follow a complex hydrodynamic trail as long as 40 m with high accuracy, even with glide phases in the trail, and can determine the direction of a trail after delays up to 35 s (Dehnhardt et al. 2001; Wieskotten et al. 2010a, 2010b). Additionally, these seals are able to follow a trail, even when they contact it at an obtuse angle, by repeatedly crossing the trail and gradually narrowing the angle. Such a search method would be more successful in tracking fleeing fish (Schulte-Pelkum et al. 2007). The beaded profile of harbor seals' vibrissae was shown to suppress self-induced vibrations caused by ambient water flow during swimming (Hanke et al. 2010). It is likely that reduced vibrations of the vibrissae allow detection of hydrodynamic trails as prey turn away from the seal during escape maneuvers. Objects of different sizes and shapes can be perceived based on characteristics of their resulting hydrodynamic trail by harbor seals' vibrissae (Wieskotten et al. 2011). Since I have shown that morphology and shape of beaded phocid vibrissae are species-specific variants on a basic pattern, the performance data from harbor seals may not be completely representative of all phocids with beaded vibrissae. The different sizes and shapes of beaded vibrissae may have functional consequences related to identifying the hydrodynamic signal of prey that have not yet been explored.

In summary, although the classic view is that pinniped vibrissae exhibit two distinct vibrissal morphologies, beaded and smooth, the morphology and shape of pinniped vibrissae within this study fall into at least three distinct groups: phocids with beaded vibrissae, phocids with smooth vibrissae, and otariids. A fourth group may be identified if additional research substantiates (with additional species and greater sample size) the division of otariid vibrissal shape into two groups as shown in our analyses. Future research should investigate further the shape differences among smooth vibrissae of otariids and phocids. Behavioral performance data for additional phocids and otariids will help elucidate the potential functional and ecological diversification that correlates with the variation in vibrissal morphology and shape reported in this study. Finally I hope to highlight the methodological insight that geometric and traditional morphometrics should not be treated as alternatives. It is fashionable to compete the two approaches to see which is "best" (e.g., Mutanen and Pretorius 2007; Parsons et al. 2003). Rather, the two types of analysis should generally be used in harmony, by fusing the data as illustrated herein, to yield the most complete understanding of morphology. In the present case, 100% of vibrissae could be classified to taxon, which is a testament to both the synthetic methodology and the biological diversity in vibrissal shape.

CHAPTER III

MATERIALS PROPERTIES

Introduction

Many organisms have developed mechanosensory structures and systems to detect physical cues in their environment (Sane and McHenry 2009). Among vertebrates, the lateral line system of fishes is among the best studied mechanosensory systems (Bleckmann 1994). The lateral line system allows an individual to receive information regarding the flow regime around its body that may originate from conspecifics (for schooling), from predators, prey or itself, as well as other biological and physical (i.e., currents) cues in its environment (Coombs and Montgomery 1999; Dijkgraaf 1962; Montgomery et al. 1995). The lateral line contains neuromast organs that transduce fluid forces to mechanoreceptors (hair cells; Dijkgraaf 1962; McHenry and van Netten 2007). Vibrissae (whiskers) are modified hairs of mammals. Pinnipeds possess vibrissae that allow them to navigate their environment and even track biogenic hydrodynamic trails in the water using this sense alone (Dehnhardt et al. 1998a; Dehnhardt et al. 2001; Gläser et al. 2011; Schulte-Pelkum et al. 2007; Wieskotten et al. 2010a, 2010b; Wieskotten et al. 2011). Traditionally, pinniped whiskers have been classified as have either smooth (with an elliptical cross-section) or beaded, with a repeating sequence of crests and troughs to give a sinusoidal profile along the length. All phocid (true or earless) seals, with the exceptions of monk (*Monachus* spp.) and bearded (*Erignathus barbatus*) seals, show the distinct beaded profile (Dehnhardt and Kaminski 1995; Ginter et al. 2010; Hyvärinen and Katajisto 1984; King 1983; Marshall et al. 2006; Ognev 1935). The vibrissae of ringed (*Pusa hispida*) and harbor (*Phoca vitulina*) seals have been observed to vibrate during swimming (Dehnhardt et al. 2001; Hyvärinen and Katajisto 1984), and this is likely true for all phocid whiskers. The beaded morphology of phocid seal vibrissae decreases these vibrations during swimming compared to smooth vibrissae, which likely increases the signal to noise ratio of vibrotactile stimuli and enhances the detection capability of mechanoreceptors in the underlying hair follicles (Hanke et al. 2010). When actively hunting, seals protract their vibrissae, which then vibrate a certain frequency based on their mechanical properties (Dehnhardt et al. 2001). Understanding the mechanical properties of vibrissal hair shafts is critical to understanding how this sensory system functions. The hair shafts of vibrissae (hereafter called vibrissae) transduce vibrotactile cues from the environmental to the mechanoreceptors deep in the vibrissal follicle-sinus complex (F-SC). Changes in its mechanical properties can modify the amplitude and frequency of vibrotactile cues that arrive at the F-SC receptors, thereby functioning as an information-processing filter. Seal vibrissae were more responsive to high frequency stimuli than cat vibrissae, and this difference was hypothesized to be related to species-specific differences in the hair shaft mechanical properties (Dykes 1975). However, the mechanical properties of vibrissal hair shafts are currently unexplored.

Vibrissae can be modeled as cantilever beams projecting from the muzzles of seals using engineering beam theory. When bent downward, the top half of a beam is placed in tension while the lower half of the beam is placed in compression (Wainwright et al. 1976). In beam theory, the neutral plane is the central plane running longitudinally through the middle of the beam that experiences no tensile or compressive stresses (force divided by cross-sectional area; Vogel 2003, Wainwright et al. 1976) during bending. Typical tension and compression elicit strains that are dependent upon material properties and are usually indifferent to the arrangement of that material (Bedford and Fowler 2004; Vogel 2003). However, calculation of bending forces, such as those generated when vibrissae are subjected to water flow, requires knowledge of both the materials properties and the geometric arrangement of the material. The geometric arrangement is referred to as the second moment of area (I) and is critical for determining the stiffness of a beam. For example, the stiffness of two rods of the same length, same diameter, same material type, and same amount of material is very different if one is solid and the other is hollow. A hollow cylinder is much stiffer than a solid rod due to the distance of the material away from the neutral plane (Vogel 2003). Here, stiffness is defined as the mechanical property that characterizes the degree of resistance of a material to deformation under a given load (Roark 1943). This measure is referred to as Young's modulus (E). Flexural stiffness is defined as a measure of the resistance of a structure to bending (Etnier 2001; Roark 1943) and is the product of Young's modulus (E) and the second moment of area (I), commonly expressed as EI (Vogel 2003; Wainwright et al. 1976). Young's modulus is a property of the material itself and is therefore assumed to remain constant over the length of a structure (Vogel 2003). Calculation of the second moment of area depends upon the cross-sectional area of the structure and this geometry can vary over the length of the beam. Often this geometry is simplified in the model. In strict engineering practices, measures of E (Young's modulus) are only valid if structures are homogeneous, isotropic, linearly elastic (Hookean), deform equally under both tensile and compressive forces, and deform less than 10% when loaded (Vogel 2003; Wainwright et al. 1976). Obviously many biological materials violate some of these assumptions, but a good estimate of flexural stiffness can be calculated if the materials testing data for the structure (i.e., vibrissae) can be collected or are available (Combes and Daniel 2003a, 2003b), and this is one goal of this study.

Chapter II of this thesis demonstrated that there is a diversity of morphologies among pinniped vibrissae. Therefore it is reasonable to assume that the flexural stiffness and mechanical properties of these vibrissae also vary. The first obvious morphological difference among pinniped vibrissae is whether they are beaded or smooth. It has been postulated that the beaded profile possessed by most phocids increases the stiffness of the "sensory lever" of these vibrissae (Yablokov and Klevezal 1964). However, I hypothesized that a beaded profile would alter the second moment of area in such a way as to reduce flexural stiffness compared to smooth vibrissae, that is smooth whiskers are stiffer than beaded whiskers. In addition, the morphology of vibrissae and behavioral studies of live pinnipeds using their vibrissae suggest that hair shaft orientation is important for sensory reception. Therefore I hypothesized that vibrissal hair shafts are not isotropic and stiffness may be greater in some orientations than others.

Materials and Methods

Vibrissae from 11 species and 43 individuals were tested (Table 4). Since there may be variation within individual pinnipeds, depending on the size of the vibrissa and its location on the muzzle, the longest vibrissae from each individual were used to standardize our comparisons. Materials properties of the vibrissae were tested using a MTS Insight 5 SL and TestWorks4 software (MTS Systems Corporation, Eden Prairie, MN). A 25N load cell (MTS Systems Corporation, Eden Prairie, MN) was equipped with a circular horizontal pin that could roll slightly to create a near frictionless contact during point force loading. Vibrissal samples were secured at the base in plastic molds filled with epoxy to keep the base stationary during testing. An apparatus that fit into the lower grip of the MTS was customized to hold each vibrissa horizontally. During testing, a point force was applied at 25% of the total length of the vibrissa minus the thickness of the epoxy base, which was calculated by:

$$L = (\text{overall whisker length} - \text{height of epoxy base})*0.25 \text{ for 25\% testing length (mm)} \quad \text{(Equation 1)}$$

This distance provided the most stable and accurate loading regime compared to other locations on the vibrissa. Using a percentage of the length allowed standardization of the testing location on vibrissae with a range of total lengths. Also, 25% is relatively close to the skin surface so the forces detected at this location may be representative of the forces experienced by the mechanoreceptors in the follicle. Lastly, this distance minimizes any potential for length errors that may arise due to worn vibrissae. The distance along the vibrissa from the epoxy mold to the point force load was used as the length of the beam (L; Equation 1) and EI was calculated over this distance to generate a measure of flexural stiffness at the point force.

$$E = \text{slope of the linear portion of the force-extension curve x } \frac{L^3}{3I} \quad \text{(Equation 2)}$$

Only the linear portion of the force-extension curve can be used to calculate E (Equation 2) because this is the only section where the material is Hookean and extension is proportional to force (Fig. 8). The assumptions of beam theory are no longer met when the slope of the graph is nonlinear. The slope of the linear portion of the graph is calculated by the equation for a line:

$$y = mx + b \text{ (Equation 3),}$$

where m is the slope. An example force-extension curve for a bearded seal vibrissa illustrates the initial linear portion used to generate the slope for the calculation of E (Fig. 8).

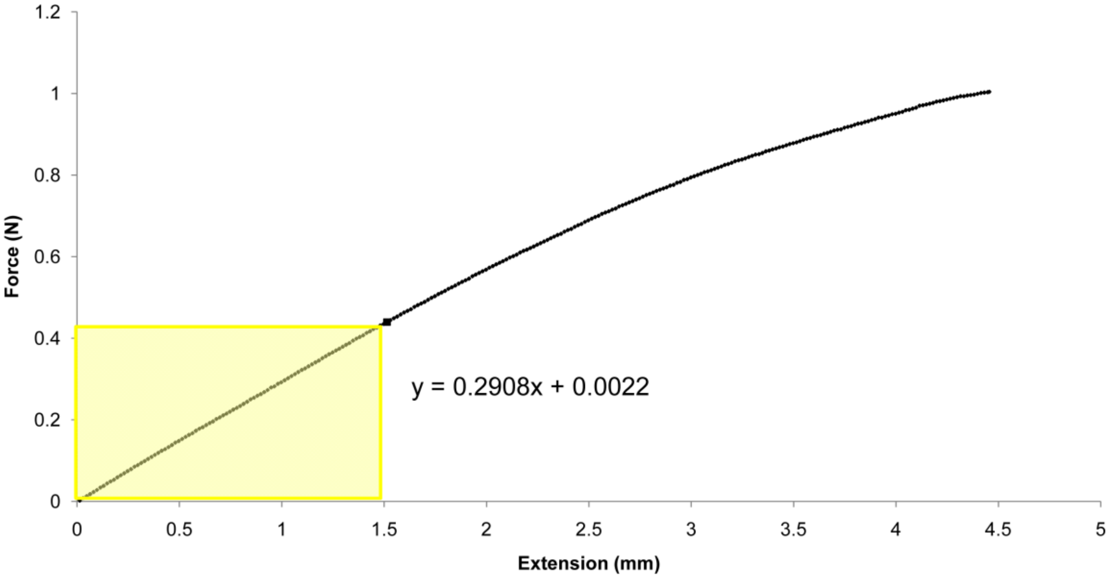

Figure 8. Example force-extension curve. A bearded seal vibrissa was tested as a cantilever beam with force (N) and extension (mm) recorded by the MTS Insight apparatus. The linear portion of the graph is highlighted in yellow. The slope of the linear portion used in calculating E is given by Equation 3. The equation for this example is shown in the figure.

Since vibrissae have an ellipsoidal cross section, the diameter of both the major and minor axes (w and h) of the ellipse at 25% of the length was measured using digital calipers (Mitutoyo Corporation, Kawasaki, Japan). The equation for the second moment of area of an ellipse with radius w in the horizontal plane and h in the vertical plane was used in calculating I:

$$I = \frac{\pi w h^3}{4} \qquad \text{(Equation 4; Wainwright et al. 1976; Vogel 2003)}$$

$I_{\text{Anterior}} = \frac{\pi w h^3}{4}$, where w = the radius of the major axis (horizontal plane) and h = the radius of the minor axis (vertical plane; Equation 5)

$I_{\text{Dorsal}} = \frac{\pi w h^3}{4}$, where w = the radius of the minor axis (horizontal plane) and h = the radius of the major axis (vertical plane; Equation 6)

The product of E, as calculated by Equation 2, and I, as calculated by Equation 5 for the anterior orientation and by Equation 6 for the dorsal orientation, resulted in the measure of flexural stiffness.

Table 4. Materials testing vibrissae samples. The number of individuals is given, classified by vibrissal profile, family and species.

Vibrissal Profile	**Family**	**Species**	**Number of Individuals**
Beaded	Phocidae	Gray seal (*Halichoerus grypus*)	5
	Phocidae	Harbor seal (*Phoca vitulina*)	5
	Phocidae	Harp seal (*Pagophilus groenlandicus*)	5
	Phocidae	Ringed seal (*Pusa hispida*)	5
	Phocidae	Spotted seal (*Phoca largha*)	5
	Phocidae	Weddell seal (*Leptonychotes weddellii*)	3
Smooth	Phocidae	Bearded seal (*Erignathus barbatus*)	5
	Otariidae	California sea lion (*Zalophus californianus*)	5
	Otariidae	Guadalupe fur seal (*Arctocephalus townsendi*)	1
	Otariidae	Northern fur seal (*Callorhinus ursinus*)	2
	Otariidae	South American fur seal (*Arctocephalus australis*)	2

Materials Testing Criteria

Several criteria were used during data collection and analysis. Since a pre-load phase was not relevant to this study, the beginning of the test was determined manually from the raw data. The test was determined to have begun when the load value no longer fluctuated to zero and the extension value was positive. To determine whether the speed of the test (how fast the crosshead was lowered) had an effect on flexural stiffness, one beaded vibrissa and one smooth vibrissa were tested at nine different test speeds ranging from 0.5mm/min to 5mm/sec. One-Way ANOVA was used to evaluate the effect of the different test speeds. The speed of the crosshead did not affect the material properties of either beaded or smooth vibrissae ($p=1.000$). These results are in agreement with a previous study which compared speeds from 10 – 100 mm/min and found no significant effect on the compressive modulus of keratinous horse hooves (Landeau et al. 1983). Based on the lack of difference among speeds observed in this study, a testing speed of 10mm/min was used throughout the rest of the trials. This speed was intermediate among those tested and decreased the time necessary for each trial (compared to the default setting).

A subset of vibrissae was tested in all four orientations: anterior, posterior, dorsal and ventral. Morphologically, as a seal swims through water, flow should contact the vibrissae at the anterior plane. Accordingly, the top of the vibrissa was denoted as the dorsal plane, the bottom as the ventral plane and the concave side as the posterior plane. Another subset of vibrissae was used to test the hypothesis that flexural stiffness was invariant whether vibrissae were wet or dry. I felt that this was important to translate the laboratory work to vibrissal function in live animals. Vibrissae were first tested in both orientations, anterior-posterior plane and dorsoventral plane, after being stored dry and then were placed in distilled water for 20 minutes. Excess water was wiped off with a paper towel and the vibrissae were immediately tested again in both orientations. In all testing scenarios, five consecutive trials were run in each orientation with the load completely removed from the vibrissa for one minute between trials.

All calculations were conducted manually in Microsoft Excel. The modulus (E) was obtained from the slope of the linear trend line fit to the raw data values on a force-extension curve using Equation 2. Variation in the flexural stiffness measurements among species and between orientations was assessed using ANOVA with species or orientation as the independent variable and flexural stiffness as the dependent variable, followed by Tukey HSD post-hoc tests in JMP software (v. 8.0.1, SAS Institute, Inc., Cary, NC). All data were log transformed to obtain normality before statistical testing. Results were determined to be statistically significant at $p<0.05$.

Results

Flexural stiffness values for the anterior and posterior planes were not significantly different from each other, nor were the values for the dorsal and ventral planes (Fig. 9). However, anterior and posterior significantly differed from dorsal and ventral for flexural stiffness ($p=0.0013$; Fig. 9). Since only two planes of the vibrissae significantly differed in flexural stiffness (anterior-posterior and dorsal-ventral), only those two planes were tested for the rest of the study. In addition, flexural stiffness values of dry vs. wet trials did not significantly differ from one another.

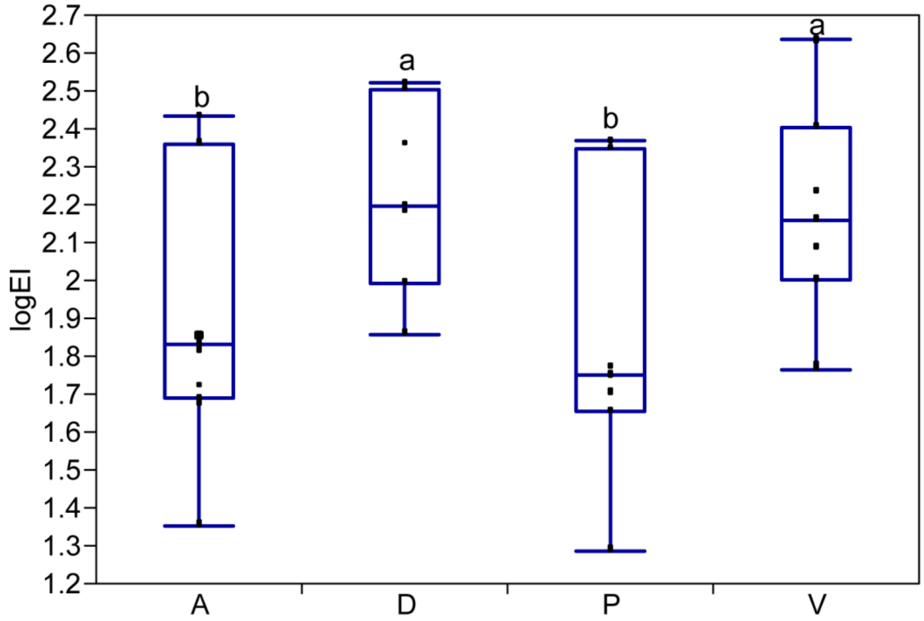

Figure 9. Results of materials testing in four orientations. A subset of pinniped vibrissae were tested in all four planes. A = Anterior, P = Posterior, D=Dorsal, V = Ventral. Dorsal and ventral did not differ from each other but had significantly higher mean flexural stiffness values than anterior and posterior, which also did not differ from each other. Different letters indicate significant differences between orientations.

For the full dataset including all species and individuals, flexural stiffness values were 1.5 to 2.9 times greater in the dorsal-ventral plane than the anterior-posterior plane ($p<0.0001$; Table 5; Fig. 10). Flexural stiffness ranged from 10.51 N/mm^2 for a ringed seal to 826.27 N/mm^2 for a fur seal in the anterior plane and from 22.61 N/mm^2 for a ringed seal to 1101.55 N/mm^2 for a fur seal in the dorsal plane.

Table 5. Results for three measurements from materials testing. Mean ± SD for Young's modulus (E), flexural stiffness (EI) and peak load is given for each species of pinniped analyzed in this study. A = anterior plane and D = Dorsal plane.

	Young's modulus (E) GPa		Flexural Stiffness (EI) N/mm^2		Peak Load (N)	
	A	D	A	D	A	D
Gray	8.15 ± 2.47	5.92 ± 1.76	34.40 ± 8.78	98.74 ± 32.36	0.10 ± 0.03	0.28 ± 0.07
Harbor	11.96 ± 1.69	7.53 ± 2.38	68.45 ± 25.88	136.47 ± 38.38	0.13 ± 0.09	0.23 ± 0.17
Harp	15.84 ± 4.21	7.62 ± 2.86	87.07 ± 44.22	152.72 ± 48.05	0.15 ± 0.05	0.27 ± 0.07
Ringed	12.06 ± 3.14	7.88 ± 2.82	40.07 ± 17.89	81.18 ± 44.72	0.07 ± 0.03	0.14 ± 0.04
Spotted	11.94 ± 1.72	5.97 ± 0.96	91.78 ± 59.51	159.12 ± 99.42	0.14 ± 0.05	0.23 ± 0.07
Weddell	8.97 ± 2.65	7.02 ± 1.05	216.54 ± 10.73	287.60 ± 23.10	0.25 ± 0.09	0.31 ± 0.09
Bearded	6.96 ± 1.81	4.85 ± 0.98	164.03 ± 79.41	433.99 ± 154.96	0.34 ± 0.20	0.81 ± 0.36
CA Sea Lion	12.23 ± 1.52	14.10 ± 5.87	171.50 ± 83.70	278.78 ± 73.52	0.34 ± 0.27	0.51 ± 0.23
Fur Seals	11.90 ± 4.06	8.94 ± 2.85	390.77 ± 229.42	590.10 ± 301.05	0.84 ± 0.40	1.20 ± 0.45

Ringed seals had the lowest flexural stiffness values and significantly differed from all species except gray seals ($p<0.0001$). Fur seals had the highest flexural stiffness values and significantly differed from all other species ($p=0.0181$; Fig. 10). The greatest difference between the two planes was observed in gray seals and the smallest difference was observed in Weddell seals (Fig. 10). The five trials of each species and in each orientation were not significantly different from each other.

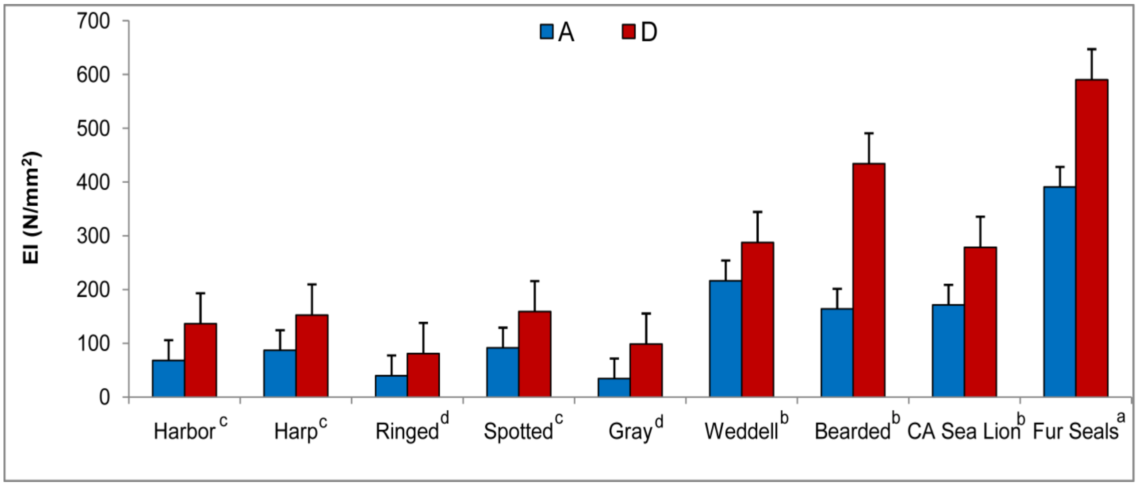

Figure 10. Results of flexural stiffness measurements (EI). Mean ± SE values are given for six species of pinnipeds with beaded vibrissae and three species with smooth vibrissae. A = Anterior plane and D = Dorsal plane. Species with different letters were significantly different.

Discussion

Pinniped vibrissae show a range of flexural stiffness values, depending on the species and the orientation of the vibrissa to the point force. Vibrissae have higher flexural stiffness values in the dorsoventral orientation, which indicates that they are more resistant to bending in that plane compared to the anterior-posterior plane. The geometry of pinniped vibrissae is clearly important since the differences in the second moment of area between the two orientations resulted in different flexural stiffness values. In the dorsal orientation, the vibrissa is much higher than it is wide so more material is located further away from the neutral axis. This should result in the structure being stiffer (Vogel 2003; Wainwright et al. 1976), and that is what was observed. The dorsal orientation resembles the engineering "ideal" structure, the I-beam, which concentrates material at the tension and compression surfaces with a minimal amount of material to hold the two surfaces apart (Wainwright et al. 1976). The pronounced differences in flexural stiffness between the two orientations likely have sensory consequences. As the animal swims forward, the vibrissae vibrate at a frequency related to their swimming speed. However, the angle of the vibrissa to the water flow also affects the vibration frequency (Hyvärinen and Katajisto 1984). The functional consequence of lower flexural stiffness in the anterior plane may be that mechanoreceptors in the underlying follicle are more sensitive to flow changes in front of the animal, as opposed to above the animal, or may result in concomitant change in mechanoreceptor distribution around the hair-shaft in the F-SC. Since many pinnipeds track prey in the water column, the anterior-posterior plane of the vibrissae may be the most important in detecting and tracking hydrodynamic trails. Orientation has been shown to affect Young's modulus in other keratinous structures. Horse-hair and porcupine quills had lower Young's modulus values when compressed in a transverse orientation, compared to a longitudinal orientation (Fraser and MacRae 1980). These data illustrate the complexity of biological structures and the necessity of testing a variety of configurations to characterize their materials properties.

The Young's modulus and flexural stiffness values reported for pinniped vibrissae in the present study are within the biological realm. A range of materials properties values for biological materials are given in Table 6. For simplicity, only keratinous structures and structures with similar diameters to pinniped vibrissae are included. Although numerous values for Young's modulus (E) and flexural stiffness (EI) are reported for biological materials, the value of E often varies depending on whether the material is tested in tension or compression. The rationale behind this phenomenon is to due heterogeneity, anisotropy and viscoelastic materials properties (MacLeod 1980). Therefore, values from tension testing are not included for comparison here. Vibrissae are composed of keratin, which has been tested in various organisms (Table 6). The modulus of keratin is approximately 5 GPa but there is a significant range around that value (Meyers et al. 2008; Wegst and Ashby 2004). Insect and spider filiform hair cuticle is a composite of several biological materials and has a Young's modulus of about 4 GPa (Dechant et al. 2001; Vincent and Wegst 2004).

Young's modulus of rat vibrissae has been reported to range from 3 - 7.36 GPa, which is comparable to pinniped vibrissae in this study (Carl et al. 2011; Hartmann et al. 2003). Flexural stiffness is less commonly reported than Young's modulus but many species of plants have been measured (Table 6). Maximum flexural stiffness for insect wings tested as cantilever beams was reported to be around $1.0\text{x}10^{-9}$ N/mm^2, which is much lower than the values reported here for pinniped vibrissae (Combes and Daniel 2003b). Butterfly wings tested as cantilever beams had EI values ranging from $2.3\text{x}10^{-14}$ to $1.49\text{x}10^{-12}$ N/mm^2 (Steppan 2000). Even lower EI values of $1.1\text{x}10^{-27}$ to $3.7\text{x}10^{-27}$ N/mm^2 were found in zebrafish larvae kinocilia (tiny hairs within the lateral line system) also tested as cantilever beams (McHenry and van Netten 2007). Flexural stiffness is likely tuned to the magnitude of forces experienced in an organism's environment, which may explain the wide range observed in biological structures. This may be particularly true for structures like vibrissae that participate in sensory systems since the materials properties affect the vibrotactile signal that reaches the sensory structures (Dykes 1975).

Table 6. Materials properties values for a range of biological structures. Diameter (mm), E (Young's modulus; GPa) and EI (flexural stiffness; N/mm^2) are given with the original reference for the data. Diameter values are only included for whole structures, values for materials that were machined to a certain diameter for testing are not included. – indicates no data for that parameter.

Material	**Diameter (mm)**	**E (GPa)**	**EI (N/mm^2)**	**Reference**
Plant stems				
Cucumber	4	–	$8.73\text{x}10^{-9}$	Vogel 1992
Daffodil	7	–	$1.19\text{X}10^{-8}$	Etnier and Vogel 2000
Horsetails	5	–	$1.87\text{x}10^{-8}$	Etnier 2003
Sedge	5	–	$7.7\text{x}10^{-9}$	Ennos 1993
Sunflower	5	–	$7.3\text{x}10^{-11}$	Vogel 1992
Tomato	5	–	$1.2\text{x}10^{-8}$	Vogel 1992
Tulip	6	–	$2.02\text{x}10^{-8}$	Etnier and Vogel 2000

Table 6, continued.

Material	**Diameter (mm)**	**E (GPa)**	**EI (N/mm^2)**	**Reference**
Plant petioles				
Banana	4 - 16	0.63 ± 0.51	$\sim 1\text{x}10^{-7}$ - $2.5\text{x}10^{-6}$	Ennos et al. 2000
Green bean	2	–	$6.77\text{x}10^{-10}$	Vogel 1992
Red maple	1	–	$1.94\text{x}10^{-10}$	Vogel 1992
Sweet gum	2	–	$9.84\text{x}10^{-10}$	Vogel 1992
White poplar	3	–	$7.75\text{x}10^{-11}$	Vogel 1992
Circular cross-section	–	1.37 – 31.9	$2.42\text{x}10^{-10}$ - $2.53\text{x}10^{-6}$	Niklas 1991
Elliptic cross-section	–	3.24 – 46.2	$2.84\text{x}10^{-10}$ - $8.44\text{x}10^{-7}$	Niklas 1991
Triangular cross-section	–	29.4 – 117.8	$5.26\text{x}10^{-9}$ - $7.47\text{x}10^{-7}$	Niklas 1991
Coral skeletons	0.7 - 4	0.0541 - 9.3	$7.31\text{x}10^{-9}$ - $1.14\text{x}10^{-7}$	Esford and Lewis 1990; Jeyasuria and Lewis 1987; Kim et al. 1992
Keratin				
Toucan beak	–	1.04 - 1.12	–	Chen et al. 2008a
Contour feather	0.67 - 1.1	0.002 - 1.85	–	MacLeod 1980
Flight feather	–	7.75-10	–	Purslow and Vincent 1978
Human hair	0.06 - 0.08	0.71 -3.63	–	Khayatt and Chamberlain 1948; Fraser and MacRae 1980
Bovine hoof	–	0.261 - 0.382	–	Franck et al. 2006
Equine hoof	–	0.523 - 2.17	–	Collins et al. 1998; Douglas et al. 1996
Horn	–	0.81 - 6.26	–	Kitchener and Vincent 1987; Li et al. 2010; Tombolato et al. 2010
Wool fiber	0.03 - 0.05	0.80 - 3.8	–	Khayatt and Chamberlain 1948
Crustacean antennae	0.4 - 2	–	$2.5\text{x}10^{-11}$ - $5.83\text{x}10^{-9}$	Etnier 2001, 2003
Crinoid arms	2	–	$5\text{x}10^{-11}$ - $3.92\text{x}10^{-10}$	Etnier 2001, 2003

Cross-sectional shape has a significant effect on the mechanical properties of biological structures. Non-circular cross-sections are relatively easier to twist (Ennos 1993; Vogel 2003, 1992). The triangular cross-section of lesser pond sedge stems and U-shaped cross-section of banana petioles results in these plants more readily twisting away from wind, rather than bending (Ennos 1993; Ennos et al. 2000). The ellipsoidal shape of pinniped vibrissal cross-sections also likely influences the bending mechanics. In a comparison of three cross-sectional shapes of plants, circular, elliptic and triangular, flexural stiffness values were similar for all three shapes but slightly greater in triangular cross-sections (Table 6; Niklas 1991). The second moment of area values provided for five species in that study were within an order of magnitude of the values calculated for pinniped vibrissae. The second moment of area was calculated in the dorsoventral and lateral (anterior-posterior) planes for pigeon feathers (Purslow and Vincent 1978). As observed here for pinniped vibrissae, I was higher in the dorsoventral plane than the lateral plane. Additionally, the maximum I values occurred at or near the insertion of the feather into the skin and decreased along the length of the feather (Purslow and Vincent 1978). However, the outermost feather was equally stiff in dorsoventral and lateral bending, while other feathers were much less stiff in the lateral plane than the dorsoventral plane. Purslow and Vincent (1978) concluded that the difference between the outermost and other feathers was because most feathers will experience the greatest force during the down stroke so greater dorsoventral stiffness is needed, but the outermost feather is the leading edge and will experience greater drag than the feathers behind it. Therefore, greater resistance to lateral bending in the outermost feather compensates for the increased drag. This indicates that the location of a structure on an organism can influence its materials properties. The complex vibrissal array of pinnipeds may show similar variation. Pinnipeds have numerous mystacial vibrissae that vary in length and diameter, as well as their location on the muzzle. This study only investigated the largest of these mystacial vibrissae. There are also several other vibrissal fields in pinnipeds (and other aquatic and terrestrial mammals), such as the rhinal and superciliary vibrissal fields, that were outside the scope of this study.

Flexural stiffness was not affected by whether the vibrissae were dry or wet. Therefore, it is reasonable to assume that the flexural stiffness values reported in this study from vibrissae which were tested dry are representative of vibrissal function in the water. Water content has previously been shown to affect the Young's modulus of biological materials, including several keratinous structures (Table 7). Tests were conducted at various hydration levels and all structures listed showed a decrease in Young's modulus with increased hydration. However, these studies have not reported effects of hydration on flexural stiffness. Orientation, and the value of I, has been shown to be of great importance in flexural stiffness. The influence of I on flexural stiffness may outweigh any changes in E and the observed lack of significant difference in flexural stiffness values between dry and wet trials may be representative of keratinous structures.

Table 7. Biological materials tested for hydration effects. Structures and the original reference are given for materials that were tested to evaluate the effects of hydration level on Young's modulus.

Material	**Structure**	**Reference**
Nacre	mollusk shell	Jackson et al. 1988
Chitin-protein	crustacean exoskeletons	Chen et al. 2008b; Hepburn et al. 1975; Joffe et al. 1975
Keratin	equine hoof wall	Bertram and Gosline 1987; Collins et al. 1998; Douglas et al. 1996; Kasapi and Gosline 1997; Meyers et al. 2008
	bovine hoof wall	Franck et al. 2006; Zhang et al. 2007
	oryx horn	Kitchener and Vincent 1987
	cattle horn	Li et al. 2010
	rhinoceros horn	Bendit and Kelly 1978
	ostrich claw	Bonser 2000; Taylor et al. 2004
	ostrich feather	Taylor et al. 2004
	toucan beak	Chen et al. 2008a
	wool	Feughelman and Robinson 1971

This is the first comparative study on the materials properties of pinniped vibrissae. The number of individuals per species was low so intraspecific variation could not be effectively assessed. However, the relatively high standard deviation values suggest that individuals may vary considerably. The results presented provide a strong foundation regarding the materials properties of pinniped vibrissae, but future studies should add to and increase the number of species, as well as the number of individuals and vibrissae per individual. Here I have characterized the flexural stiffness of pinniped vibrissae at one location. Flexural stiffness may change along the length of the vibrissa as the structure tapers. However, hydrodynamic trail-following relies on vibrotactile stimuli being transmitted to the mechanoreceptors by the hair shaft. Therefore, testing locations near the base (i.e., 25% of total length) may be more indicative of the mechanical function that allows these tracking behaviors than locations near the tip of the vibrissa. The vibrissae of many species are worn down with use so testing at 25% gave greater confidence that homologous locations were tested in this comparative study than would distances closer to the tip of the vibrissae. Additionally, studies on other biological materials have had difficulty obtaining data near the tip of the structure due to slippage (Combes and Daniel 2003a), and this is also true for pinniped vibrissae. The material properties of the tips of such structures may best be estimated using methods such as Finite Element Modeling.

Much research on pinniped vibrissae has focused on the differences in shape between some phocids, which demonstrate a sinusoidal beaded profile, and the remaining phocids, otariids and odobenids, which have a smooth vibrissal profile (i.e., Chapter II of this thesis). It was hypothesized that a beaded profile would alter the second moment of area in such a way as to reduce flexural stiffness compared to smooth vibrissae, which was supported by the results of this testing. Smooth vibrissae generally demonstrated higher flexural stiffness values than beaded vibrissae. Intuitively, it would seem more likely that vibrissae with higher flexural stiffness values could be kept protracted in a flow more easily. However, since the beaded profile has been shown to reduce vibrations (Hanke et al. 2010), it is possible that these vibrissae can be kept protracted in flow without an increase in stiffness that could reduce their sensitivity to small changes in flow. The captive animal performance data has shown that harbor seals with beaded vibrissae have a higher success rate in tracking hydrodynamic trails than California sea lions with smooth vibrissae (Dehnhardt et al. 1998a; Dehnhardt et al. 2001; Gläser et al. 2011; Schulte-Pelkum et al. 2007; Wieskotten et al. 2010a, 2010b; Wieskotten et al. 2011). The higher flexural stiffness values observed in smooth vibrissae may make these structures less able to detect small deflections from changes in flow created by a swimming prey item. It was surprising that bearded seals did not show higher flexural stiffness values since they use smooth vibrissae in active touch behavior while foraging on the benthos (Burns 1981; Marshall et al. 2006). Walruses are also benthic foragers and their vibrissae have been described as the "toughest" of the pinnipeds (Berta et al. 2006). Otariid (sea lions and fur seals) vibrissae have been observed to grow to greater lengths than phocid vibrissae (Bonner 1968; Hirons et al. 2001; King 1983; Ling 1966). A longer structure must be stiffer than a shorter structure of the same material to support its own weight. Therefore, the higher flexural stiffness values of otariid vibrissae may be a compensation for their generally greater overall length. It is also possible that the materials properties of smooth vibrissae are tuned for active touch behaviors, such as benthic foraging and social interactions with conspecifics, and the different materials properties of beaded vibrissae are tuned for passive touch behaviors, such as hydrodynamic reception. The results of this study indicate that the materials properties of pinniped vibrissae may be just as important as the morphological profile in vibrissal function. The hydrodynamic performance of these sensory structures is complex and we are just beginning to understand the function of vibrissae for sensory perception in pinnipeds.

CHAPTER IV

CONCLUSIONS

Summary

How pinniped vibrissae function as tactile sensors to detect prey has been investigated from many angles. Follicle-sinus complexes in pinnipeds have a large investment of innervation that indicates the importance of this sensory system to this taxonomic group. Research from both captive and wild pinnipeds have provided ample evidence for the use of vibrissae in searching for prey and tracking hydrodynamic trails. However, previous studies had not comparatively addressed the vibrissal hair shafts (vibrissae) themselves. As stated previously the shape and material properties of the vibrissae are critical to transducing environmental cues to the sensory functional units within the F-SCs. Surprisingly, research focusing on this component of vibrissae is sparse to non-existent. The overall goal of this thesis was to not only provide additional data on vibrissae but to do so from a comparative perspective, which also has been lacking in the literature.

The results of this study greatly advance our knowledge of how pinniped vibrissal sensory systems function. Additionally, I presented a new combined morphometrics analysis that integrates traditional and geometric morphometrics. This combined approach successfully created a more complete, quantified description of pinniped vibrissal shape, and has widespread application within the field of functional morphology. Species-specific differences in traditional morphometric measurements had been shown previously (Ginter et al. 2010) and those differences were maintained in the present study. Phocids with beaded vibrissae show species-specific variation on a common sinusoidal beaded pattern. In all analyses, the phocids possessing beaded vibrissae clustered together. It was expected that species with smooth vibrissae (bearded seals and otariids) would cluster together in morphospace. However, the centroid ellipses for bearded seals and otariids never overlapped in the geometric morphometric or the combined data analysis. The interesting differences among pinnipeds with smooth vibrissae, which were previously assumed to be the same, were a surprising result of this study. Another unexpected finding was that gray seals appeared to be more similar to bearded seals in morphospace despite the fact that they showed the relatively "bumpiest" vibrissae. The combined approach used true rank scaling of both traditional morphometric measurements and principal components of elliptic Fourier harmonic coefficients to combine the datasets that were originally measured in different units. This approach proved to be the most powerful in discriminating among species and correctly classified 100% of individuals to taxon. It also demonstrated the redundancy between traditional and geometric morphometrics, suggesting that these two approaches should be combined, rather than used independently, for a complete analysis of shape.

This study is the first attempt to characterize the materials properties of pinniped vibrissae. The Young's modulus and flexural stiffness values reported here for pinniped vibrissae are within the biological realm, though high for their size. Pinniped vibrissae showed a range of flexural stiffness values, depending on the species and the orientation of the vibrissa to the point force. Gray seal vibrissae showed the greatest difference between the two orientations and Weddell seal vibrissae showed the smallest difference. The orientation of the vibrissa to the point force was a significant effect in all species tested but only two out of the four planes of the vibrissae were significantly different in flexural stiffness. The dorsal orientation always had a higher flexural stiffness value than the anterior orientation, which suggests that the vibrissae are tuned to be more flexible laterally than dorsoventrally. This difference may also relate to the distribution of mechanoreceptors around the hair shaft in the underlying follicle. Projected sensory structures, such as vibrissae and antennae, must keep a fine balance between being too stiff so that even small stimuli jar the organism, and not being stiff enough so that small stimuli go unnoticed (Loudon 2005). Pinnipeds tracking prey in the water column need vibrissae that are stiff enough to remain protracted in a flow, but not so stiff that they might miss small perturbations caused by the hydrodynamic trail of a prey item swimming nearby. The anterior plane is the surface of the vibrissae which receives most of the pressure from flow as the animal swims but it is also likely the plane that detects flow changes from hydrodynamic trails. The fact that the anterior orientation was always relatively less stiff than the dorsal orientation suggests that displacement in the lateral plane may be more informative than displacement in the dorsoventral plane. These results demonstrate that the differences in shape among pinniped vibrissae are not the only factor which affects their hydrodynamic function. There may be an optimal combination of shape and flexural stiffness for sensory perception. The shape of beaded vibrissae may create less turbulent flow around them that could interfere with detection of hydrodynamic stimuli. Since this morphology has been shown to reduce vibrations (Hanke et al. 2010), it is possible that these vibrissae can be kept protracted while the animal is swimming without an increase in stiffness that could reduce their sensitivity to small changes in flow. There is likely a complex interaction between shape and stiffness of pinniped vibrissae that has functional implications for their sensory ecology.

Recommendations for Future Work

Although a large number of Phocidae species were sampled, it was primarily members of subfamily Phocinae. Future studies should augment these data by including more species from the Monachinae subfamily, particularly elephant (*Mirounga* spp.) seals, as the deepest diving pinnipeds, and monk (*Monachus* spp.) seals, which are phocids with smooth vibrissae. Ross seals are also a Monachine species of interest due to some discrepancy in the literature as to whether these phocids have beaded or smooth vibrissae. Additional otariid samples would help clarify the possible existence of a fourth vibrissal morphology, in addition to smooth, beaded and bearded seals. Walruses, as the only living odobenid, are interesting for several reasons. Their foraging and vibrissal distribution differ from other pinnipeds, with the exception of bearded seals, and their vibrissae are much shorter and wider than the vibrissae of any pinniped investigated here. These shape differences which are obvious by eye need to be quantified. It is possible that the vibrissae of walruses and bearded seals are convergent as a result of similar foraging modes. Therefore, it could be anticipated that walruses might cluster with bearded seals in a discriminant function analysis. Gray seals stood out in both the morphological and materials properties analyses. They separated from the beaded cluster in morphospace and were positioned almost intermediate between the beaded phocids and bearded seals. Their vibrissae also showed the greatest anisotropy in flexural stiffness. Such interesting characteristics point toward the need for additional performance and ecological investigation on the natural history of gray seals. As usual, research often generates just a many questions as it answers.

Future work on the mechanical function of vibrissae will involve measuring flexural stiffness at additional locations along the vibrissa. Since otariid vibrissae were stiffer than phocid vibrissae, further testing of additional otariid individuals and species is needed to explore this trend. Walruses have vibrissae which are quite different from otariids and phocids. Walruses' vibrissae are much shorter and wider than otariid or phocid vibrissae and also considerably more numerous; walruses have approximately ten times or more as many vibrissae as most phocids and otariids (King 1983; Ling 1977; Yablokov and Klevezal 1964). Bearded seals are the only species analyzed to date which comes close to walruses in number of vibrissae, with about twice as many as the highest number for other phocids (Marshall et al. 2006). Further biomechanical studies of pinniped vibrissae should incorporate flow tank testing and DPIV (digital particle image velocimetry) to quantitatively measure flow changes around beaded and smooth vibrissae. These methods have already been used to show that the beaded morphology of harbor seal vibrissae decrease vibrations compared to smooth vibrissae (Hanke et al. 2010). However, since the discriminant function analyses (Chapter II) separated all individuals to taxon, the beaded morphology of harbor seals is not identical to other species. Therefore, it will be important to quantify the flow around vibrissae from other species to determine how exactly the beaded morphologies affect flow around the vibrissae. The captive animal studies have been almost exclusively performed on harbor seals and California sea lions. This study has shown that these species differ from other beaded and smooth-whiskered species, respectively, in both morphology and materials properties. Comparative captive animal testing using the same methodology should illustrate whether the observed differences in morphology and materials properties affect the way the animal uses these structures while tracking hydrodynamic trails in the water.

This study has laid a methodological groundwork for further comparative work on pinniped vibrissal morphology and materials properties. All analyses showed interesting differences between species that likely have functional consequences. The effects of vibrissal morphology and materials properties on the ecology of pinnipeds are currently unknown. Additional comparative analyses are needed to quantify these effects in terms of the phylogeny, foraging ecology and life history of pinnipeds.

LITERATURE CITED

ADAMS, D. C., F. J. ROHLF, AND D. E. SLICE. 2004. Geometric morphometrics: Ten years of progress following the 'revolution', Italian Journal of Zoology 71:5-16.

AHL, A. S. 1986. The role of vibrissae in behavior: A status review, Veterinary Research Communications 10:245-268.

AU, W. W. L. 2008. Echolocation, Pp. 348-357 in Encyclopedia of Marine Mammals (W. F. Perrin, B. Würsig and J. G. M. Thewissen, eds.). Academic Press, New York, NY.

BEDFORD, A. M., AND W. FOWLER. 2004. Engineering Mechanics: Statics and Dynamics, 4th ed. Prentice Hall, Upper Saddle River, NJ.

BENDIT, E. G., AND M. KELLY. 1978. Properties of the matrix in keratins. Part I: The compression testing technique, Textile Research Journal 48:674-679.

BERTA, A., J. L. SUMICH, AND K. M. KOVACS. 2006. Marine Mammals: Evolutionary Biology, 2nd ed. Academic Press, San Diego, CA.

BERTRAM, J. E., AND J. M. GOSLINE. 1987. Functional design of horse hoof keratin: The modulation of mechanical properties through hydration effects, Journal of Experimental Biology 130:121-136.

BLECKMANN, H. 1994. Reception of hydrodynamic stimuli in aquatic and semiaquatic animals, Progress in Zoology 41:1-115.

BLECKMANN, H., T. BREITHAUPT, R. BLICKHAN, AND J. TAUTZ. 1991. The time course and frequency content of hydrodynamic events caused by moving fish, frogs, and crustaceans, Journal of Comparative Physiology A: Neuroethology, Sensory, Neural, and Behavioral Physiology 168:749-757.

BLICKHAN, R., C. KRICK, D. ZEHREN, W. NACHTIGALL, AND T. BREITHAUPT. 1992. Generation of a vortex chain in the wake of a undulatory swimmer, Naturwissenschaften 79:220-221.

BODIG, J., AND B. A. JAYNE. 1982. Mechanics of Wood and Wood Composites. Van Nostrand Reinhold Company, New York, NY.

BONESS, D. J., W. D. BOWEN, AND O. T. OFTEDAL. 1994. Evidence of a maternal foraging cycle resembling that of otariid seals in a small phocid, the harbor seal, Behavioral Ecology and Sociobiology 34:95-104.

BONNER, W. N. 1968. The fur seal of South Georgia, British Antarctic Survey Scientific Reports 56:1-81.

BONSER, R. H. C. 2000. The Young's modulus of ostrich claw keratin, Journal of Materials Science Letters 19:1039-1040.

BURGESS, P., AND E. PERL. 1973. Cutaneous mechanoreceptors and nociceptors, Pp. 29-78 in Handbook of Sensory Physiology 2: Somatosensory System (A. Iggo, ed.). Springer-Verlag, Berlin.

BURNS, J. J. 1981. Bearded seal *Erignathus barbatus* Erxleben, 1777, Pp. 145-170 in Handbook of Marine Mammals (S. H. Ridgway and R. J. Harrison, eds.). Academic Press, London.

BURNS, J. M., S. J. TRUMBLE, M. A. CASTELLINI, AND J. W. TESTA. 1998. The diet of Weddell seals in McMurdo Sound, Antarctica as determined from scat collections and stable isotope analysis, Polar Biology 19:272-282.

CAMERON, A. W. 1967. Breeding behavior in a colony of western Atlantic gray seals, Canadian Journal of Zoology 45:161-173.

CANNELL, M. G. R., AND J. MORGAN. 1987. Young's modulus of sections of living branches and tree trunks, Tree Physiology 3:355-364.

CARL, K., W. HILD, J. MAMPEL, C. SCHILLING, R. UHLIG, AND H. WITTE. 2011. Characterisation of statical properties of rat's whisker system, IEEE Sensors Journal (accepted), doi: 10.1109/JSEN.2011.2114341.

CHEN, P. Y., A. Y. M. LIN, Y. S. LIN, Y. SEKI, A. G. STOKES, ET AL. 2008a. Structure and mechanical properties of selected biological materials, Journal of the Mechanical Behavior of Biomedical Materials 1:208-226.

CHEN, P. Y., A. Y. M. LIN, J. MCKITTRICK, AND M. A. MEYERS. 2008b. Structure and mechanical properties of crab exoskeletons, Acta Biomaterialia 4:587-596.

COLLINS, S. N., B. C. COPE, L. HOPEGOOD, R. J. LATHAM, R. G. LINFORD, AND J. D. REILLY. 1998. Stiffness as a function of moisture content in natural materials: Characterisation of hoof horn samples, Journal of Materials Science 33:5185-5191.

COMBES, S. A., AND T. L. DANIEL. 2003a. Flexural stiffness in insect wings I. Scaling and the influence of wing venation, Journal of Experimental Biology 206:2979-2987.

COMBES, S. A., AND T. L. DANIEL. 2003b. Flexural stiffness in insect wings II. Spatial distribution and dynamic wing bending, Journal of Experimental Biology 206:2989-2997.

COOMBS, S., AND J. C. MONTGOMERY. 1999. The enigmatic lateral line system, Pp. 319-362 in Comparative Hearing: Fish and Amphibians (R. R. Fay and A. N. Popper, eds.). Springer, New York, NY.

CRAIG, R. G., F. A. PEYTON, AND D. W. JOHNSON. 1961. Compressive properties of enamel, dental cements, and gold, Journal of Dental Research 40:936-945.

DARROCH, J. N., AND J. E. MOSIMANN. 1985. Canonical and principal components of shape, Biometrika 72:241-252.

DAVIS, R. W., ET AL. 1999. Hunting behavior of a marine mammal beneath the Antarctic fast ice, Science 283:993-995.

DECHANT, H. E., F. RAMMERSTORFER, AND F. BARTH. 2001. Arthropod touch reception: stimulus transformation and finite element model of spider tactile hairs, Journal of Comparative Physiology A: Neuroethology, Sensory, Neural, and Behavioral Physiology 187:313-322.

DEHNHARDT, G. 1994. Tactile size discrimination by a California sea lion (*Zalophus californianus*) using its mystacial vibrissae, Journal of Comparative Physiology A: Neuroethology, Sensory, Neural, and Behavioral Physiology 175:791-800.

DEHNHARDT, G., AND A. KAMINSKI. 1995. Sensitivity of the mystacial vibrissae of harbour seals (*Phoca vitulina*) for size differences of actively touched objects, Journal of Experimental Biology 198:2317-2323.

DEHNHARDT, G., AND G. DÜCKER. 1996. Tactual discrimination of size and shape by a California sea lion (*Zalophus californianus*), Learning & Behavior 24:366-374.

DEHNHARDT, G., AND B. MAUCK. 2008. Mechanoreception in secondarily aquatic vertebrates, Pp. 295-314 in Sensory Evolution on the Threshold: Adaptations in Secondarily Aquatic Vertebrates (J. G. M. Thewissen and S. Nummela, eds.). University of California Press, Berkeley, CA.

DEHNHARDT, G., B. MAUCK, AND H. BLECKMANN. 1998a. Seal whiskers detect water movements, Nature 394:235-236.

DEHNHARDT, G., B. MAUCK, AND H. HYVÄRINEN. 1998b. Ambient temperature does not affect the tactile sensitivity of mystacial vibrissae in harbour seals, Journal of Experimental Biology 201:3023-3029.

DEHNHARDT, G., H. HYVÄRINEN, A. PALVIAINEN, AND G. KLAUER. 1999. Structure and innervation of the vibrissal follicle sinus complex in the Australian water rat, *Hydromys chrysogaster*, Journal of Comparative Neurology 411:550-562.

DEHNHARDT, G., B. MAUCK, W. HANKE, AND H. BLECKMANN. 2001. Hydrodynamic trail-following in harbor seals (*Phoca vitulina*), Science 293:102-104.

DIJKGRAAF, S. 1962. The functioning and significance of the lateral line organs, Biological Reviews 38:51-105.

DOUGLAS, J. E., C. MITTAL, J. J. THOMASON, AND J. C. JOFRIET. 1996. The modulus of elasticity of equine hoof wall: Implications for the mechanical function of the hoof, Journal of Experimental Biology 199:1829-1836.

DRUCKER, E. G., AND G. V. LAUDER. 1999. Locomotor forces on a swimming fish: Three-dimensional vortex wake dynamics quantified using digital particle image velocimetry, Journal of Experimental Biology 202:2393.

DYKES, R. W. 1975. Afferent fibers from mystacial vibrissae of cats and seals, Journal of Neurophysiology 38**:**650-662.

ENNOS, A. R. 1993. The mechanics of the flower stem of the sedge *Carex acutiformis*, Annals of Botany 72**:**123-127.

ENNOS, A. R., H.-C. SPATZ, AND T. SPECK. 2000. The functional morphology of the petioles of the banana, *Musa textilis*, Journal of Experimental Botany 51**:**2085-2093.

ESFORD, L. E., AND J. C. LEWIS. 1990. Stiffness of Caribbean gorgonians (Coelenterata, Octocorallia) and Ca/Mg content of their axes, Marine Ecology Progress Series 67**:**189-200.

ETNIER, S. A. 2001. Flexural and torsional stiffness in multi-jointed biological beams, Biological Bulletin 200**:**1-8.

ETNIER, S. A. 2003. Twisting and bending of biological beams: Distribution of biological beams in a stiffness mechanospace, Biological Bulletin 205**:**36-46.

ETNIER, S. A., AND S. VOGEL. 2000. Reorientation of daffodil (Narcissus: Amaryllidaceae) flowers in wind: Drag reduction and torsional flexibility, American Journal of Botany 87**:**29-32.

FAY, F. H. 1982. Ecology and biology of the Pacific walrus, *Odobenus rosmarus divergens* Illiger, North American Fauna 74**:**1-279.

FEUGHELMAN, M., AND M. S. ROBINSON. 1971. Some mechanical properties of wool fibers in the" Hookean" region from zero to 100% relative humidity, Textile Research Journal 41**:**469-474.

FISH, F. E., L. E. HOWLE, AND M. M. MURRAY. 2008. Hydrodynamic flow control in marine mammals, Integrative and Comparative Biology 48:788-800.

FRANCK, A., G. COCQUYT, P. SIMOENS, AND N. DE BELIE. 2006. Biomechanical properties of bovine claw horn, Biosystems Engineering 93**:**459-467.

FRASER, R. D., AND T. P. MACRAE. 1980. Molecular structure and mechanical properties of keratins, Pp. 211-246 in The Mechanical Properties of Biological

Materials, Symposium of the Society for Experimental Biology (J. F. V. Vincent and J. D. Currey, eds.). Cambridge University Press, Cambridge.

GINTER, C. C., F. E. FISH, AND C. D. MARSHALL. 2010. Morphological analysis of the bumpy profile of phocid vibrissae, Marine Mammal Science 26**:**733-743.

GLÄSER, N., S. WIESKOTTEN, C. OTTER, G. DEHNHARDT, AND W. HANKE. 2011. Hydrodynamic trail following in a California sea lion (*Zalophus californianus*), Journal of Comparative Physiology A: Neuroethology, Sensory, Neural, and Behavioral Physiology 197**:**141-151.

GOODMAN-LOWE, G. D. 1998. Diet of the Hawaiian monk seal (*Monachus schauinslandi*) from the Northwestern Hawaiian islands during 1991 to 1994, Marine Biology 132**:**535-546.

GOTTSCHALDT, K. M., A. IGGO, AND D. W. YOUNG. 1973. Functional characteristics of mechanoreceptors in sinus hair follicles of the cat, Journal of Physiology 235**:**287-315.

GREAVES, D. K., M. O. HAMMILL, J. D. EDDINGTON, D. PETTIPAS, AND J. F. SCHREER. 2004. Growth rate and shedding of vibrissae in the gray seal, *Halichoerus grypus*: A cautionary note for stable isotope diet analysis, Marine Mammal Science 20**:**296-304.

HALATA, Z. 1975. The mechanoreceptors of the mammalian skin ultrastructure and morphological classification, Pp. 5-75 in Advances in Anatomy, Embryology and Cell Biology (A. Brodal, W. Hild, J. van Limborgh, R. Ortmann, T. H. Schiebler, et al., eds.). Springer-Verlag, New York, NY.

HALATA, Z., AND B. L. MUNGER. 1980. Sensory nerve endings in rhesus monkey sinus hairs, Journal of Comparative Neurology 192**:**645-663.

HANKE, F. D., AND G. DEHNHARDT. 2009. Aerial visual acuity in harbor seals (*Phoca vitulina*) as a function of luminance, Journal of Comparative Physiology A: Neuroethology, Sensory, Neural, and Behavioral Physiology 195**:**643-650.

HANKE, F. D., W. HANKE, C. SCHOLTYSSEK, AND G. DEHNHARDT. 2009. Basic mechanisms in pinniped vision, Experimental Brain Research 199:299-311.

HANKE, F. D., C. SCHOLTYSSEK, W. HANKE, AND G. DEHNHARDT. 2011. Contrast sensitivity in a harbor seal (*Phoca vitulina*), Journal of Comparative Physiology A: Neuroethology, Sensory, Neural, and Behavioral Physiology 197:203-210.

HANKE, W., AND H. BLECKMANN. 2004. The hydrodynamic trails of *Lepomis gibbosus* (Centrarchidae), *Colomesus psittacus* (Tetraodontidae) and *Thysochromis ansorgii* (Cichlidae) investigated with scanning particle image velocimetry, Journal of Experimental Biology 207:1585-1596.

HANKE, W., C. BRUCKER, AND H. BLECKMANN. 2000. The ageing of the low-frequency water disturbances caused by swimming goldfish and its possible relevance to prey detection, Journal of Experimental Biology 203:1193-1200.

HANKE, W., M. WITTE, L. MIERSCH, M. BREDE, J. OEFFNER, ET AL. 2010. Harbor seal vibrissa morphology suppresses vortex-induced vibrations, Journal of Experimental Biology 213:2665-2672.

HARTMANN, M. J., N. J. JOHNSON, R. B. TOWAL, AND C. ASSAD. 2003. Mechanical characteristics of rat vibrissae: Resonant frequencies and damping in isolated whiskers and in the awake behaving animal, Journal of Neuroscience 23:6510-6519.

HEPBURN, H. R., I. JOFFE, N. GREEN, AND K. J. NELSON. 1975. Mechanical properties of a crab shell, Comparative Biochemistry and Physiology Part A: Physiology 50:551-554.

HINDELL, M. A., D. J. SLIP, AND H. R. BURTON. 1991. The diving behavior of adult male and female Southern elephant seals, *Mirounga leonina* (Pinnipedia, Phocidae), Australian Journal of Zoology 39:595-619.

HIRONS, A. C., D. M. SCHELL, AND D. J. ST. AUBIN. 2001. Growth rates of vibrissae of harbor seals (*Phoca vitulina*) and Steller sea lions (*Eumetopias jubatus*), Canadian Journal of Zoology 79**:**1053-1061.

HYVÄRINEN, H. 1989. Diving in darkness: Whiskers as sense organs of the ringed seal (*Phoca hispida saimensis*), Journal of Zoology 218**:**663-678.

HYVÄRINEN, H. 1995. Structure and function of the vibrissae of the ringed seal (*Phoca hispida* L.), Pp. 429–445 in Sensory Systems of Aquatic Mammals (R. A. Kastelein, J. A. Thomas and P. E. Nachtigall, eds.). De Spil Publishers, Woerden, The Netherlands.

HYVÄRINEN, H., AND H. KATAJISTO. 1984. Functional structure of the vibrissae of the ringed seal (*Phoca hispida* Schr.), Acta Zoologica Fennica 171**:**17-30.

JACKSON, A. P., J. F. V. VINCENT, AND R. M. TURNER. 1988. The mechanical design of nacre, Proceedings of the Royal Society of London. Series B. Biological sciences 234**:**415-440.

JACKSON, D. A. 1993. Stopping rules in principal components analysis: A comparison of heuristical and statistical approaches, Ecology 74**:**2204-2214.

JEYASURIA, P., AND J. C. LEWIS. 1987. Mechanical properties of the axial skeleton in gorgonians, Coral Reefs 5**:**213-219.

JOFFE, I., H. R. HEPBURN, K. J. NELSON, AND N. GREEN. 1975. Mechanical properties of a crustacean exoskeleton, Comparative Biochemistry and Physiology Part A: Physiology 50**:**545-549.

KASAPI, M. A., AND J. M. GOSLINE. 1997. Design complexity and fracture control in the equine hoof wall, Journal of Experimental Biology 200**:**1639-1659.

KASTELEIN, R. A., AND M. A. VAN GAALEN. 1988. The sensitivity of the vibrissae of a Pacific walrus (*Odobenus rosmarus divergens*), Aquatic Mammals 14**:**123-133.

KHAYATT, R. M., AND N. H. CHAMBERLAIN. 1948. The bending modulus of animal fibres, Journal of the Textile Institute Transactions 39**:**185-197.

KIM, K., W. M. GOLDBERG, AND G. T. TAYLOR. 1992. Architectural and mechanical properties of the black coral skeleton (Coelenterata: Antipatharia): A comparison of two species, The Biological Bulletin 182:195-209.

KING, J. E. 1969. Some aspects of the anatomy of the Ross seal: *Ommatophoca rossi* (Pinnipedia: Phocidae), British Antarctic Survey Scientific Reports 63:1-77.

KING, J. E. 1983. Seals of the World, 2nd ed. British Museum (Natural History), London.

KITCHENER, A., AND J. F. V. VINCENT. 1987. Composite theory and the effect of water on the stiffness of horn keratin, Journal of Materials Science 22:1385-1389.

KUHL, F. P., AND C. R. GIARDINA. 1982. Elliptic Fourier features of a closed contour, Computer Graphics and Image Processing 18:236-258.

LANDEAU, L. J., D. J. BARRETT, AND S. C. BATTERMAN. 1983. Mechanical properties of equine hooves, American Journal of Veterinary Research 44:100-102.

LE BOEUF, B. J., D. E. CROCKER, D. P. COSTA, S. B. BLACKWELL, P. M. WEBB, AND D. S. HOUSER. 2000. Foraging ecology of northern elephant seals, Ecological Monographs 70:353-382.

LEVENSON, D. H., AND R. J. SCHUSTERMAN. 1997. Pupillometry in seals and sea lions: Ecological implications, Canadian Journal of Zoology 75:2050-2057.

LEVENSON, D. H., AND R. J. SCHUSTERMAN. 1999. Dark adaptation and visual sensitivity in shallow and deep-diving pinnipeds, Marine Mammal Science 15:1303-1313.

LI, B. W., H. P. ZHAO, X. Q. FENG, W. W. GUO, AND S. C. SHAN. 2010. Experimental study on the mechanical properties of the horn sheaths from cattle, Journal of Experimental Biology 213:479-486.

LICHTENSTEIN, S. H., G. E. CARVELL, AND D. J. SIMONS. 1990. Responses of rat trigeminal ganglion neurons to movements of vibrissae in different directions, Somatosensory & Motor Research 7:47-65.

LINDT, C. C. 1956. Underwater behavior of the southern sea lion, *Otaria jubata*, Journal of Mammalogy 37:287-288.

LING, J. K. 1966. The skin and hair of the southern elephant seal, *Mirounga leonina* (Linn.) I. The facial vibrissae, Australian Journal of Zoology 14:855-866.

LING, J. K. 1972. Vibrissa follicles of the Ross seal, British Antarctic Survey Bulletin 27:19-24.

LING, J. K. 1977. Vibrissae of marine mammals, Pp. 387-415 in Functional Anatomy of Marine Mammals (R. J. Harrison, ed.). Academic Press, London.

LONGENECKER, K. 2010. Fishes in the Hawaiian monk seal diet, based on regurgitate samples collected in the Northwestern Hawaiian Islands, Marine Mammal Science 26:420-429.

LOUDON, C. 2005. Flexural stiffness of insect antennae, American Entomologist 51:48-49.

MACLEOD, G. D. 1980. Mechanical properties of contour feathers, Journal of Experimental Biology 87:65-71.

MARSHALL, C. D., H. AMIN, K. M. KOVACS, AND C. LYDERSEN. 2006. Microstructure and innervation of the mystacial vibrissal follicle-sinus complex in bearded seals, *Erignathus barbatus* (Pinnipedia: Phocidae), The Anatomical Record Part A 288A:13-25.

MARSHALL, C. D., G. D. HUTH, V. M. EDMONDS, D. L. HALIN, AND R. L. REEP. 1998. Prehensile use of perioral bristles during feeding and associated behaviors of the Florida manatee (*Trichechus manatus latirostris*), Marine Mammal Science 14:274-289.

MARSHALL, C. D., H. MAEDA, M. IWATA, M. FURUTA, S. ASANO, ET AL. 2003. Orofacial morphology and feeding behaviour of the dugong, Amazonian, West African and Antillean manatees (Mammalia: Sirenia): Functional morphology of the muscular-vibrissal complex, Journal of Zoology 259:245-260.

MAUCK, B., U. EYSEL, AND G. DEHNHARDT. 2000. Selective heating of vibrissal follicles in seals (*Phoca vitulina*) and dolphins (*Sotalia fluviatilis guianensis*), Journal of Experimental Biology 203**:**2125-2131.

MCHENRY, M. J., AND S. M. VAN NETTEN. 2007. The flexural stiffness of superficial neuromasts in the zebrafish (*Danio rerio*) lateral line, Journal of Experimental Biology 210**:**4244-4253.

MCLELLAN, T., AND J. A. ENDLER. 1998. The relative success of some methods for measuring and describing the shape of complex objects, Systematic Biology 47**:**264.

MENCUCCINI, M., J. GRACE, AND M. FIORAVANTI. 1997. Biomechanical and hydraulic determinants of tree structure in Scots pine: Anatomical characteristics, Tree Physiology 17**:**105-113.

MEYERS, M. A., P. Y. CHEN, A. Y. M. LIN, AND Y. SEKI. 2008. Biological materials: Structure and mechanical properties, Progress in Materials Science 53**:**1-206.

MIKLOSOVIC, D. S., M. M. MURRAY, L. E. HOWLE, AND F. E. FISH. 2004. Leading-edge tubercles delay stall on humpback whale (*Megaptera novaeangliae*) flippers, Physics of Fluids 16**:**L39-L42.

MILLER, E. H. 1975. A comparative study of facial expressions of two species of pinnipeds, Behaviour 270**:**268-284.

MILLER, E. H., AND D. J. BONESS. 1979. Remarks on display functions of the snout of the grey seal, *Halichoerus grypus* (Fab.), with comparative notes, Canadian Journal of Zoology 57**:**140-148.

MITCHINSON, B., K. N. GURNEY, P. REDGRAVE, C. MELHUISH, A. G. PIPE, ET AL. 2004. Empirically inspired simulated electro-mechanical model of the rat mystacial follicle-sinus complex, Proceedings of the Royal Society of London. Series B: Biological Sciences 271**:**2509-2516.

MONTGOMERY, J., S. COOMBS, AND M. HALSTEAD. 1995. Biology of the mechanosensory lateral line in fishes, Reviews in Fish Biology and Fisheries 5:399-416.

MUTANEN, M., AND E. PRETORIUS. 2007. Subjective visual evaluation vs. traditional and geometric morphometrics in species delimitation: A comparison of moth genitalia, Systematic Entomology 32:371-386.

NEIMARK, M. A., M. L. ANDERMANN, J. J. HOPFIELD, AND C. I. MOORE. 2003. Vibrissa resonance as a transduction mechanism for tactile encoding, Journal of Neuroscience 23:6499-6509.

NEWBY, T. C., F. M. HART, AND R. A. ARNOLD. 1970. Weight and blindness of harbor seals, Journal of Mammalogy 51:152.

NIKLAS, K. J. 1991. Flexural stiffness allometries of angiosperm and fern petioles and rachises: Evidence for biomechanical convergence, Evolution 45:734-750.

OGNEV, S. 1935. Mammals of the USSR and Adjacent Countries. Vol. III, Carnivora (Fissipedia and Pinnipedia). Academy of Sciences USSR, Moscow.

OLIVER, G. W. 1977. Navigation in mazes by a grey seal, *Halichoerus grypus* (Fabricius), Behaviour 67:97-114.

PARRISH, F. A., M. P. CRAIG, T. J. RAGEN, G. J. MARSHALL, AND B. M. BUHLEIER. 2000. Identifying diurnal foraging habitat of endangered Hawaiian monk seals using a seal-mounted video camera, Marine Mammal Science 16:392-412.

PARSONS, K. J., B. W. ROBINSON, AND T. HRBEK. 2003. Getting into shape: An empirical comparison of traditional truss-based morphometric methods with a newer geometric method applied to New World cichlids, Environmental Biology of Fishes 67:417-431.

PAULY, D., A. W. TRITES, E. CAPULI, AND V. CHRISTENSEN. 1998. Diet composition and trophic levels of marine mammals, ICES Journal of Marine Science 55:467-481.

PAVLICEV, M., G. P. WAGNER, AND J. M. CHEVERUD. 2009. Measuring evolutionary constraints through the dimensionality of the phenotype: Adjusted bootstrap method to estimate rank of phenotypic covariance matrices, Evolutionary Biology 36:339-353.

PLÖTZ, J., H. BORNEMANN, R. KNUST, A. SCHRÖDER, AND M. BESTER. 2001. Foraging behaviour of Weddell seals, and its ecological implications, Polar Biology 24:901-909.

POLKEY, W., AND W. N. BONNER. 1966. The pelage of the Ross seal, British Antarctic Survey Bulletin 8:93-96.

PURSLOW, P. P., AND J. F. V. VINCENT. 1978. Mechanical properties of primary feathers from the pigeon, Journal of Experimental Biology 72:251-260.

REEP, R. L., C. D. MARSHALL, M. L. STOLL, AND D. M. WHITAKER. 1998. Distribution and innervation of facial bristles and hairs in the Florida manatee (*Trichechus manatus latirostris*), Marine Mammal Science 14:257-273.

REEP, R. L., M. L. STOLL, C. D. MARSHALL, B. L. HOMER, AND D. A. SAMUELSON. 2001. Microanatomy of facial vibrissae in the Florida manatee: The basis for specialized sensory function and oripulation, Brain, Behavior and Evolution 58:1-14.

RICE, F. L., AND B. L. MUNGER. 1986. A comparative light microscopic analysis of the sensory innervation of the mystacial pad. II. The common fur between the vibrissae, Journal of Comparative Neurology 252:186-205.

RICE, F. L., A. MANCE, AND B. L. MUNGER. 1986. A comparative light microscopic analysis of the sensory innervation of the mystacial pad. I. Innervation of vibrissal follicle sinus complexes, Journal of Comparative Neurology 252:154-174.

RICE, F. L., B. T. FUNDIN, J. ARVIDSSON, H. ALDSKOGIUS, AND O. JOHANSSON. 1997. Comprehensive immunofluorescence and lectin binding analysis of vibrissal follicle sinus complex innervation in the mystacial pad of the rat, Journal of Comparative Neurology 385:149-184.

ROARK, R. J. 1943. Formulas for Stress and Strain, 2nd ed. McGraw-Hill, New York, NY.

ROHLF, F. J. 1993. EFAWin. Department of Ecology and Evolution, State University of New York at Stony Brook, Stony Brook, NY.

ROHLF, F. J. 2004. tpsDig2. Department of Ecology and Evolution, State University of New York at Stony Brook, Stony Brook, NY.

ROHLF, F. J., AND L. F. MARCUS. 1993. A revolution in morphometrics, Trends in Ecology and Evolution 8**:**129-132.

SALMAN, A., M. BILECENOGLU, AND H. GÜÇLÜSOY. 2001. Stomach contents of two Mediterranean monk seals (*Monachus monachus*) from the Aegean Sea, Turkey, Journal of the Marine Biological Association of the United Kingdom 81**:**719-720.

SANE, S. P., AND M. J. MCHENRY. 2009. The biomechanics of sensory organs, Integrative and Comparative Biology 49**:**1-16.

SCHEFFER, V. B. 1962. Pelage and surface topography of the northern fur seal, North American Fauna 64**:**1-206.

SCHEINER, S. M. 2001. MANOVA: Multiple response variables and multispecies interactions, Pp. 99-115 in Design and Analysis of Ecological Experiments (S. M. Scheiner and J. Gurevitch, eds.). Oxford University Press, New York, NY.

SCHOLTYSSEK, C., A. KELBER, AND G. DEHNHARDT. 2008. Brightness discrimination in the harbor seal (*Phoca vitulina*), Vision Research 48**:**96-103.

SCHULTE-PELKUM, N., S. WIESKOTTEN, W. HANKE, G. DEHNHARDT, AND B. MAUCK. 2007. Tracking of biogenic hydrodynamic trails in harbour seals (*Phoca vitulina*), Journal of Experimental Biology 210**:**781-787.

SCHUSTERMAN, R. J. 1981. Behavioral capabilities of seals and sea lions: a review of their hearing, visual, learning and diving skills, Psychological Record 31**:**125-143.

SCHUSTERMAN, R. J., W. N. KELLOGG, AND C. E. RICE. 1965. Underwater visual discrimination by the California sea lion, Science 147**:**1594-1596.

SCHUSTERMAN, R. J., D. KASTAK, D. H. LEVENSON, C. J. REICHMUTH, AND B. L. SOUTHALL. 2000. Why pinnipeds don't echolocate, Journal of the Acoustical Society of America 107:2256-2264.

STEPHENS, R. J., I. J. BEEBE, AND T. C. POULTER. 1973. Innervation of the vibrissae of the California sea lion, *Zalophus californianus*, The Anatomical Record 176:421-441.

STEPPAN, S. J. 2000. Flexural stiffness patterns of butterfly wings (Papilionoidea), Journal of Research on the Lepidoptera 35:61-77.

TAYLOR, A. M., R. H. C. BONSER, AND J. W. FARRENT. 2004. The influence of hydration on the tensile and compressive properties of avian keratinous tissues, Journal of Materials Science 39:939-942.

TOMBOLATO, L., E. E. NOVITSKAYA, P. Y. CHEN, F. A. SHEPPARD, AND J. MCKITTRICK. 2010. Microstructure, elastic properties and deformation mechanisms of horn keratin, Acta Biomaterialia 6:319-330.

VICKERMAN, J. C., AND I. S. GILMORE. 2009. Surface Analysis: The Principal Techniques. John Wiley & Sons, New York, NY.

VINCENT, J. F. V., AND U. G. K. WEGST. 2004. Design and mechanical properties of insect cuticle, Arthropod Structure and Development 33:187-199.

VOGEL, S. 1992. Twist-to-bend ratios and cross-sectional shapes of petioles and stems, Journal of Experimental Botany 43:1527-1532.

VOGEL, S. 2003. Comparative Biomechanics: Life's Physical World. Princeton University Press, Princeton, NJ.

WAINWRIGHT, S. A., W. D. BIGGS, J. D. CURREY, AND J. M. GOSLINE. 1976. Mechanical Design in Organisms. Princeton University Press, Princeton, NJ.

WARTZOK, D. 1984. Seal echolocation?, Nature 308:753.

WARTZOK, D., AND G. C. RAY. 1976. A verification of Weber's law for visual discrimination of disc sizes in the Bering Sea spotted seal, *Phoca largha*, Vision Research 16:819-822.

WARTZOK, D., AND M. G. MCCORMICK. 1978. Color discrimination by a Bering Sea spotted seal, *Phoca largha*, Vision Research 18:781-784.

WARTZOK, D., R. ELSNER, H. STONE, B. P. KELLY, AND R. W. DAVIS. 1992. Under-ice movements and the sensory basis of hole finding by ringed and Weddell seals, Canadian Journal of Zoology 70:1712-1712.

WATKINS, W. A., AND D. WARTZOK. 1985. Sensory biophysics of marine mammals, Marine Mammal Science 1:219-260.

WEGST, U. G. K., AND M. F. ASHBY. 2004. The mechanical efficiency of natural materials, Philosophical Magazine 84:2167-2186.

WEIFFEN, M., B. MÖLLER, B. MAUCK, AND G. DEHNHARDT. 2006. Effect of water turbidity on the visual acuity of harbor seals (*Phoca vitulina*), Vision Research 46:1777-1783.

WIESKOTTEN, S., G. DEHNHARDT, B. MAUCK, L. MIERSCH, AND W. HANKE. 2010a. Hydrodynamic determination of the moving direction of an artificial fin by a harbour seal (*Phoca vitulina*), Journal of Experimental Biology 213:2194-2200.

WIESKOTTEN, S., G. DEHNHARDT, B. MAUCK, L. MIERSCH, AND W. HANKE. 2010b. The impact of glide phases on the trackability of hydrodynamic trails in harbour seals (*Phoca vitulina*), Journal of Experimental Biology 213:3734-3740.

WIESKOTTEN, S., B. MAUCK, L. MIERSCH, G. DEHNHARDT, AND W. HANKE. 2011. Hydrodynamic discrimination of wakes caused by objects of different size or shape in a harbour seal (*Phoca vitulina*), Journal of Experimental Biology 214:1922-1930.

WINN, H. E., AND N. E. REICHLEY. 1985. Humpback whale *Megaptera novaeangliae* (Borowski, 1781), Pp. 241-273 in Handbook of Marine Mammals (S. H. Ridgway and R. Harrison, eds.). Academic Press, London.

YABLOKOV, A. V., AND G. A. KLEVEZAL. 1964. Vibrissae of whales and seals, their distribution, structure and significance, Pp. 48–81 in Morphological

Features of Aquatic Mammals (S. E. Kleynenberg, ed.). The Science Publishing House, Moscow.

ZHANG, D., D. D. AROLA, R. K. REPROGEL, W. ZHENG, U. TASCH, AND R. M. DYER. 2007. A method for characterizing the mechanical behaviour of hoof horn, Journal of Materials Science 42**:**1108-1115.

VITA

Name: Carly C. Ginter

Address: c/o Dr. Christopher Marshall
200 Seawolf Pkwy
OCSB 112
Galveston, TX 77553

Email Address: ccginter@hotmail.com

Education: B.S., Biology, West Chester University, 2009
M.S., Wildlife and Fisheries Sciences, Texas A&M University, 2011

Publications: GINTER, C. C., T. J. DEWITT, F. E. FISH, AND C. D. MARSHALL. Fused traditional and geometric morphometrics demonstrate pinniped whisker diversity. Submitted to PLoS ONE.

GINTER, C. C., S. A. BÖTTGER, AND F. E. FISH. 2011. Morphology and microanatomy of harbor porpoise (*Phocoena phocoena*) dorsal fin tubercles, Journal of Morphology 272**:**27-33.

GINTER, C. C., F. E. FISH, AND C. D. MARSHALL. 2010. Morphological analysis of the bumpy profile of phocid vibrissae, Marine Mammal Science 26**:**733-743.